CEN - 133 (B)

FIESTA

A ONE DIMENSIONAL, TWO GROUP SPACE-TIME KINETICS CODE FOR CALCULATING PWR SCRAM REACTIVITIES

NOVEMBER, 1979

POWER SYSTEMS
COMBUSTION ENGINEERING INC

LEGAL NOTICE

ABSTRACT

This report describes FIESTA, a one-dimensional two-group space-time kinetics computer code. The intended use of this code is for PWR scram reactivity calculations which account for the axial space-time variations in the neutron flux. The use of space-time reactivities reduces the margin requirements for transients sensitive to scram reactivity characteristics compared to the use of static reactivities which do not account for delayed neutron effects. The FIESTA code is used for these calculations instead of the HERMITE code previously approved by NRC mainly for two reasons: (1) FIESTA calculations are more rapid than HERMITE ones, and (2) FIESTA produces kinetics parameters which are readily used for point kinetics calculations.

The FIESTA code has been verified with HERMITE and with comparisons of standard benchmark problems. Although the code has been written to incorporate feedback on fuel temperature and moderator density, such feedbacks are not needed for scram reactivity calculations. A code input description is included in the Appendix.

TABLE OF CONTENTS

APPENDICES

1.0 Introduction

It is standard practice in the nuclear industry to calculate the time dependent reactivity insertion by calculating the critical eigenvalue as a function of rod position. This type of calculation assumes that the neutron flux shape during a scram rod insertion is equal to the critical flux shape at each rod position. Such an assumption is conservative since the critical (or static) flux shape tends to shift away from the rods more than space-time calculation would predict, and hence result in smaller reactivity insertion. The primary reason for the difference in the flux shape is that the delayed neutron precursors are distributed according to the initial neutron flux shape, and as the neutron population decreases the importance of the precursors increases. The neutron precursors provide a source of neutrons which tends to tilt the neutron flux shape toward the rods compared to static methods, and hence leads to greater reactivity insertion at intermediate rod positions.

This effect tends to become large at the end of a reactor cycle when the power shape tends to be axially flat. At certain intermediate rod positions, for example, the reactivity change predicted by static methods may be only half or a third of the reactivity predicted by space-time methods. At full rod insertions both methods yield nearly the same reactivity.

2.0 FIESTA Model

FIESTA is a one-dimensional, 2 group space-time kinetics code which allows up to six delayed neutron precursor groups. The model is based on a space-time factorization method which divides the neutron flux into a time-dependent amplitude function times a time-dependent shape function. This method is useful since it reduces the number of times that the flux shape must be re-evaluated and permits ready computations of reactivity components.

Section 2.1 describes the neutron kinetics model. The first part of which is a general derivation of the kinetics equations and a development of the equations which are solved by the space-time factorization method. The second part applies the resulting equations to the two energy group model.

2.1 Time Dependent Neutron Diffusion Equation Space-Time Factorization Method

The space-time factorization method presented in this section is identical to the improved quasistatic method presented by Ott et al (Ref. 2.1). The term "quasistatic" is avoided in this report since it is sometimes used to refer to the adiabatic method* (Ref. 2.2).

The general time dependent neutron diffusion equation may be written as follows:

$$\frac{1}{v(E)}\frac{\partial\phi(r,E,t)}{\partial t} = \nabla\cdot D(r,E,t)\,\nabla\phi(r,E,t)$$

$$- \Sigma_T(r,E,t)\phi(r,E,t) + \int dE'\Sigma_s(r,E'',t)\, f(r,E'\to E)\,\phi(r,E',t)$$

$$+ \sum_j f_p^j(E) \int dE'(1-\beta^j)\,\nu^j(E')\,\Sigma_f^j(r,E',t)\,\phi(r,E',t)$$

$$+ \sum_i f_d^i(E)\,\lambda_i C_i(r,t) \qquad 2.1.1$$

$$\frac{\partial C_i(r,t)}{\partial t} = -\lambda_i C_i(r,t) + \sum_j \int dE'\,\beta_i^j\nu^j(E')\,\Sigma_f(r,E',t)\,\phi(r,E',t)$$

*The adiabatic method assumes that flux shapes correspond to the static flux shapes of the perturbed reactor state. The space-time factorization method is an exact method, in that the solution approaches the exact solution for sufficiently small time steps since all time derivatives are retained in this formulation. The adiabatic method does not have this property since the solution for the flux shape neglects all time derivatives.

where the definition of terms is as follows:

$\phi(r,E,t)$ - is the neutron flux at position r, energy E and time t

$D(r,E,t)$ - is the diffusion coefficient

$\Sigma_T(r,E,t)$ - is the total cross section

$\nu\Sigma_f(r,E,t)$ - is nu times the fission cross section

$\Sigma_s(r,E,t)$ - is the scattering cross section

$f_s(r,E' \rightarrow E)$ - is the scattering kernel at position r

$f_p^j(E)$ - is the prompt neutron spectrum

∇ - denotes the spatial gradient

$f_d^i(E)$ - is the delayed neutron spectrum of delayed group (i)

β_i^j - is the delayed neutron fraction of group (i) resulting from fissionable isotope (j)

λ_i - is the decay constant of delayed group (i)

$C_i(r,t)$ - is the concentration of precursors of delayed group (i)

The following definition is applied in the space-time factorization method

$$\phi(r,E,t) \equiv T(t) \; \psi(r,E,t) \qquad 2.1.2$$

The motivation for this definition is to place most of the time variation of the neutron flux into the amplitude function T(t).

This definition introduces an additional variable, and therefore an additional equation is required. The following normalization equation is chosen:

$$\int dE \int dr \; \psi_0^+(r,E) \; \psi(r,E,t) \; \frac{1}{v(E)} = \text{constant} \qquad 2.1.3$$

where $\psi_0^+(r,E)$ is the initial steady state adjoint flux. The value of the constant is determined by the initial flux, since the initial amplitude is assumed to be equal to unity

$$\psi(r,E,t)\Big|_{t=0} = \phi_0(r,E)$$

The time dependent neutron diffusion equation may be written in the following short notation

$$\frac{1}{v}\frac{\partial \phi}{\partial t} = L\phi + \sum_i \lambda_i \overset{*}{C}_i$$

$$\frac{\partial \overset{*}{C}_i}{\partial t} = -\lambda_i \overset{*}{C}_i + H_i \phi \qquad 2.1.4$$

where $\phi = \phi(r,E,t)$

$\overset{*}{C}_i = C_i(r,E,t)\, f_d^i(E)$

L and H_i are operators whose form may be obtained from Equation 2.1.1 and Equation 2.1.2.

Substituting Equation 2.1.2 into the above equation, multiplying by the adjoint and integrating over space and energy, the following is obtained:

$$\frac{\partial}{\partial t}\left\langle \psi_0^+ \frac{\psi T}{v} \right\rangle = T\langle \psi_0^+ L\psi \rangle + \sum \lambda_i \langle \psi_0^+ \overset{*}{C}_i \rangle$$

$$\frac{\partial}{\partial t}\langle \psi_0^+ \overset{*}{C}_i \rangle = -\langle \psi_0^+ \overset{*}{C}_i \lambda_i \rangle + \langle \psi_0^+ H_i \psi \rangle T$$

where $T = T(t)$ is the flux amplitude

$\lambda = \lambda(r,E,t)$ is the flux shape function

$\lambda_0^+ = \psi_0^+(r,E)$ is the initial adjoint flux

$\langle\rangle$ signifies integration over space and energy

These equations may be arranged into a form identical to the Point-Kinetics equations.

$$\frac{\partial T}{\partial t} = \frac{\rho - \beta}{\Lambda} T + \sum_i \lambda_i K_i$$

$$\frac{\partial K_i}{\partial t} = -\lambda_i K_i + \frac{\beta}{\Lambda} T$$

where $K_i(t) = \dfrac{\langle \psi_0^+(r,E)\, f_d^i(E)\, C_i(r,t) \rangle}{\langle \psi_0^+(r,E)\, \frac{1}{v}(E)\, \psi(r,E,t) \rangle}$

$$\frac{\beta_i}{\Lambda}(t) = \frac{\langle \Psi_0^+ H_i \Psi \rangle}{\langle \Psi_0^+ \frac{\Psi}{v} \rangle}$$

$$\frac{\rho}{\Lambda}(t) = \frac{\langle \Psi_0^+ L\Psi \rangle}{\langle \Psi_0^+ \frac{\Psi}{v} \rangle} + \sum_{i=1}^{I} \frac{\langle \Psi_0^+ H_i \Psi \rangle}{\langle \Psi_0^+ \frac{\Psi}{v} \rangle}$$

Space-time behavior is retained with these equations since the shape function is time varying. The Point-Kinetics restriction ($\Psi(r,E,t) = \Psi_0(r,E)$) is not applied with this method (i.e., ρ/Λ and β/Λ depend on the flux shape). These equations are non-linear and cannot be solved directly since the shape function is not known.

To obtain the shape function, Equation 2.1.4 is considered again. The precursor concentration may be solved directly since it depends only on the flux history prior to the time of interest.

$$\overset{*}{C}_i(r,t) = \overset{*}{C}_{i_0}(r)e^{-\lambda_i t} + \int dE \int_0^t d\tau H_i(r,E,\tau)\ \phi(r,E,\tau)e^{-\lambda_i(t-\tau)} \qquad 2.1.6$$

The neutron diffusion equation may be written as follows:

$$\frac{1}{v} T \frac{\partial \Psi}{\partial t} + \frac{1}{v} \Psi \frac{\partial T}{\partial t} = LT\Psi + \Sigma \lambda_i \overset{*}{C}_i$$

Since the flux shape is a slowly varying function, the following approximation is made

$$\left.\frac{\partial \Psi}{\partial t}\right|_{t=t^\ell} = \frac{\Psi^\ell - \Psi^{\ell-1}}{\Delta t^\ell} \qquad 2.1.7$$

This approximation results in the improved quasistatic method which has been shown to be accurate compared to exact results by Meneley, et al (Ref. 2.3). The equation for the shape may then be written at time level (ℓ)

$$M^\ell(r,E)\ \Psi^\ell(r,E) + S^\ell(r,E) = 0 \qquad 2.1.8$$

where $M^\ell = T^\ell \{L^\ell - \frac{1}{v}\frac{1}{T^\ell}\left.\frac{\partial T}{\partial t}\right|_{t=t^\ell} - \frac{1}{v\Delta t^\ell}\}$

$$S^\ell = \sum_i \lambda_i \overset{*}{C}_i + \frac{T^\ell}{v}\frac{\Psi^{\ell-1}}{\Delta t^\ell}$$

L^{ℓ} is the diffusion operator at the new time level (ℓ) which is known unless there is feedback. For feedback an iteration procedure is required.

$T^{\ell}, \left.\frac{dT}{dt}\right|^{\ell}$ are the amplitude and the time derivative of the amplitude at the new time level. These quantities are unknown, but approximate values may be used which yield good results.

The solution to the shape equation is then reduced to a fixed source problem.

It can be seen that the space-time factorization method is an alternate method of time differencing the kinetics equations. Instead of time differencing the <u>total</u> flux, the amplitude and the flux shape are time differenced, separately, with different time step sizes. Since the flux shape is more slowly varying than the amplitude, a larger time step size may be chosen for the former. In addition, since the flux shape between time levels may be assumed to be constant, the Point-Kinetics approximation is used in this time range. The space-time factorization method, therefore, introduces an additional variable (T) and an additional equation (Point-Kinetics Equation). An overall saving may be realized, however, since the shape equation, which is the most time consuming calculation, may be evaluated less frequently than with the normal space-time differencing procedures.

<u>Kinetics Parameters and Adjoint Weighting</u>

The general form of the kinetics parameters is:

$$\rho(t) = \frac{1}{F(t)} \langle \psi_0^+(r,E)\, L_\rho(r,E,t)\, \psi(r,E,t) \rangle$$

$$\beta_i(t) = \frac{1}{F(t)} \langle \psi_0^+(r,E)\, L_{\beta_i}(r,E,t)\, \psi(r,E,t) \rangle$$

$$\Lambda(t) = \frac{1}{F(t)} \langle \psi_0^+(r,E)\, \frac{1}{v(E)}\, \psi(r,E,t) \rangle \qquad 2.1.9$$

where F(t) is an arbitrary function which is normally taken as the fission source.

$$F(t) = \sum_j \langle \psi_0^+(r,E)\, v\Sigma_f^j(r,E,t)\, \psi(r,E,t) \rangle$$

$L_\rho(r,E,t)$ is the reactivity operator

$L_{\beta_i}(r,E,t)$ is the delayed neutron operator

$$L_\rho(r,E,t)\,\Psi(r,E,t) \equiv \nabla \cdot D(r,E,t)\,\nabla\Psi(r,E,t)$$

$$-\Sigma_T(r,E,t)\,\Psi(r,E,t) + \int dE'\,\Sigma_s(r,E',t)\,f_j(r,E'\to E)\,\Psi(r,E',t)$$

$$+ \sum_j f_p^j(E) \int dE'(1-\beta^j)\,\nu\Sigma_f^j(r,E',t)\,\Psi(r,E',t)$$

$$+ \sum_i \sum_j f_d^i(E) \int dE'\,\beta_i^j\,\nu\Sigma_f^j(r,E',t)\,\Psi(r,E',t)$$

$$L_{\beta i}(r,E,t)\,\Psi(r,E,t) \equiv \sum_j f_d^{ij}(E) \int dE'\beta_i^j\,\nu\Sigma_f^j(r,E',t)\,\Psi(r,E',t) \qquad 2.1.10$$

The reactivity operator may be simplified somewhat by making use of the initial steady state condition

$$L_{\rho_0}(r,E)\,\Psi_0(r,E) = 0 \qquad 2.1.11$$

A similar expression may be written for the adjoint flux.

$$L^+_{\rho_0}(r,E)\,\Psi^+_0(r,E) = 0 \qquad 2.1.12$$

where the adjoint operator is defined by:

$$\langle \Psi^+ L_\rho \Psi \rangle \equiv \langle \Psi L^+_\rho \Psi^+ \rangle \qquad 2.1.13$$

The reactivity operator and the flux may be expanded.

$$L_\rho(r,E,t) \to L_{\rho_0}(r,E) + \delta L_\rho(r,E,t) \qquad 2.1.14$$

$$\Psi(r,E,t) = \Psi_0(r,E) + \delta\Psi(r,E,t)$$

The reactivity may then be written as the sum of four terms

$$\rho(t) = \frac{1}{F(t)} \langle \Psi_0^+ L_{\rho_0} \Psi_0 \rangle$$

$$+\frac{1}{F(t)} \langle \Psi_0^+ L_{\rho_0} \delta\Psi \rangle$$

$$+ \frac{1}{F(t)} \langle \Psi_0^+ \delta L_\rho \Psi_0 \rangle$$

$$+ \frac{1}{F(t)} \langle \Psi_0^+ \delta L_\rho \delta\Psi \rangle$$

The first term vanishes from the steady state condition Equation 2.1.1. The second term vanishes since

$$< \Psi_0^+ L_{\rho_0} \delta\Psi > = < \delta\Psi L_{\rho_0}^+ \Psi_0^+ > = 0$$

Only two terms remain

$$\rho(t) = \frac{1}{F(t)} <\Psi_0^+ \delta L_\rho \Psi_0> + \frac{1}{F(t)} <\Psi_0^+ \delta L_\rho \delta\Psi >$$

2.1.15

The first term is the normal Point Kinetics* Reactivity Component and the second term is the space-time contribution to the reactivity (Reactivity introduced due to flux shape changes). The latter will be referred to as the Flux-Shape-Reactivity-Component throughout this report.

The above discussion illustrates the reason why the kinetics parameters are usually adjoint weighted. An arbitrary weighting factor could be chosen without introducing any error. The choice of the adjoint, however, eliminates first order errors in the calculated reactivity due to errors in the flux shape. Space-time effects are minimized, or conversely, the time range over which the Point-Kinetics approximation is valid has been extended.

The reactivity components can be sub-divided further into the various contributors.

$$L_\rho \rightarrow \underset{\text{rod motion}}{L_\rho} + \underset{\text{moderator feedback}}{L_\rho} + \underset{\text{Doppler feedback}}{L_\rho}$$

The Point-Kinetics-Reactivity-Component and the Flux-Shape-Reactivity Component can each be subdivided into these three separate reactivity components.

*Normally the Point Kinetics Reactivity is calculated with $F(t) = F_o$. The above definition is retained, however, to preserve the additive property of the reactivity components. This is a good approximation since only small variations in F(t) are expected.

2.1.2 Two Group Reactor Kinetics Equations

Space-Time Factorization Method

The general kinetics results are reduced to two energy groups in this section.

The diffusion equation is reduced to two energy groups by integrating over a finite energy range.

$$\frac{1}{v_1}\frac{\partial \phi_1(r,t)}{\partial t} = \nabla\cdot D_1(r,t)\,\nabla\phi_1(r,t) - \{\Sigma_{a_1}(r,t) + \Sigma_r(r,t)\}\;\phi_1(r,t)$$

$$+ (1-\beta)\,\nu\Sigma_{f_1}(r,t)\,\phi_1(r,t) + (1-\beta)\,\nu\Sigma_{f_2}(r,t)\,\phi_2(r,t)$$

$$+ \sum_i \lambda_i C_i(r,t)$$

$$\frac{1}{v_2}\frac{\partial \phi_2(r,t)}{\partial t} = \nabla\cdot D_2(r,t)\,\nabla\phi_2(r,t) - \Sigma_{a_2}(r,t)\,\phi_2(r,t)$$

$$+ \Sigma_r(r,t)\,\phi_1(r,t)$$

$$\frac{\partial C_i(r,t)}{\partial t} = -\lambda_i C_i(r,t) + \beta_i\{\nu\Sigma_{f_1}(r,t)\,\phi_1(r,t) + \nu\Sigma_{f_2}(r,t)\,\phi_2(r,t)\} \qquad 2.1.16$$

where:

$$\phi_g(r,t) = \int_g dE\;\phi(r,E,t)$$

$$\frac{1}{v_g}(r,t) = \frac{1}{\phi_g(r,t)}\int_g dE\;\frac{1}{v(E)}\,\phi(r,E,t)$$

$$D_g(r,t) = \frac{1}{\nabla\phi_g(r,t)}\int_g dE\;D(r,E,t)\;\nabla\phi(r,E,t)$$

$$\Sigma_{ag}(r,t) = \frac{1}{\phi_g(r,t)}\int_g dE\;\Sigma_a(r,E,t)\,\phi(r,E,t)$$

$$\Sigma_r(r,t) = \frac{1}{\phi_1(r,t)}\int_{g_2} dE \int_{g_1} dE'\;\Sigma_s(r,E',t)\,f_s(r,E'\to E)\,\phi(r,E',t)$$

$$\nu\Sigma_{fg}(r,t) = \frac{1}{\phi_g(r,t)} \sum_j \int_g dE\ \nu\Sigma_f^j(r,E,t)\ \phi(r,E,t)$$

$$\beta_i(r,t) = \frac{\sum_j dE'\ \beta_i^j\ \nu\Sigma_f^i(r,E',t)\ \phi(r,E',t)}{\sum_j dE'\ \nu\Sigma_f^j(r,E',t)\ \phi(r,E',t)}$$

It is assumed that the spectrum within each group is constant, so that these cross-sections are not time dependent as a result of spectrum changes. (The cross-sections are, however, time dependent as a result of feedback.)

It also has been assumed that all delayed neutrons are identical in spectrum to the prompt neutrons and that all prompt and delayed neutrons are born in the fast energy group.

$$\int_{g_1} dE f_d^i(E) = \int_{g_1} dE f_p^j(E) = 1$$

$$\int_{g_2} dE f_d^i(E) = \int_{g_2} dE f_p^i(E) = 0$$

The difference in spectrum between prompt and delayed neutrons is not distinguishable in a two energy group model. (The difference in spectrum between the prompt and the delayed neutrons is often taken into account by calculating a modified delayed neutron fraction (β-effective). Detailed discussion of this calculation may be found elsewhere (Ref. 2.4).

Equation 2.1.16 may be written in a short notation

$$\frac{1}{v_1}\frac{\partial\phi_1}{\partial t} = L_1\phi_1 + M_1\phi_2 + \sum_i \lambda_i C_i$$

$$\frac{1}{v_2}\frac{\partial\phi_2}{\partial t} = L_2\phi_2 + M_2\phi_1$$

$$\frac{\partial C_i}{\partial t} = -\lambda_i C_i + \beta_i \{R_1\phi_1 + R_2\phi_2\} \qquad 2.1.17$$

The Space-Time Factorization method is applied

$$\phi_1(r,t) = T(t)\ \Psi_1(r,t)$$

$$\phi_2(r,t) = T(t)\,\Psi_2(r,t) \qquad 2.1.18$$

and substituted into the above equation. This process yields the amplitude equation (Equation 2.1.5) as shown in the previous section.

The kinetics parameters are modified from the previous results to reflect the use of the two group approximation

$$\rho(t) = \frac{1}{F(t)} \{ \langle \Psi_{10}^{+} \nabla\cdot D_1 \nabla\Psi_1 \rangle - \langle \Psi_{10}^{+} \Sigma_{a_1} \Psi_1 \rangle$$

$$- \langle \Psi_{10}^{+} \Sigma_r \Psi_1 \rangle + \langle \Psi_{10}^{+} \nu\Sigma_{f_1} \Psi_1 \rangle$$

$$+ \langle \Psi_{10}^{+} \nu\Sigma_{f_2} \Psi_2 \rangle + \langle \Psi_{20}^{+} \nabla\cdot D_2 \Psi_2 \rangle$$

$$- \langle \Psi_{20}^{+} \Sigma_{a_2} \Psi_2 \rangle \}$$

$$\beta_i(t) = \frac{1}{F(t)} \sum_j \beta_i^j \{ \langle \Psi_{10}^{+} \nu\Sigma_{f_1}^j \Psi_1 \rangle + \langle \Psi_{10}^{+} \nu\Sigma_{f_2}^j \Psi_2 \rangle \}$$

$$\Lambda(t) = \frac{1}{F(t)} \{ \langle \Psi_{10}^{+} \frac{1}{v_1} \Psi_1 \rangle + \langle \Psi_{20}^{+} \frac{1}{v_2} \Psi_2 \rangle \}$$

$$F(t) = \sum_j \{ \langle \Psi_{10}^{+} \nu\Sigma_{f_1}^j \Psi_1 \rangle + \langle \Psi_{10}^{+} \nu\Sigma_{f_2} \Psi_2 \rangle \} \qquad 2.1.19$$

It is assumed the delayed neutron fractions may be precalculated for specific fissioning isotopes in the core and that the delayed neutron fraction is time independent.

The shape equation may be written in two energy groups

$$\left\{-L_1^{\ell} + \frac{1}{v_1 T^{\ell}} \left.\frac{\partial T}{\partial t}\right|_{t=t^{\ell}} + \frac{1}{v_1 \Delta t^{\ell}}\right\} \psi_1^{\ell} - M_1^{\ell} \psi_2^{\ell} = \frac{\Sigma \lambda_i C_i}{T} + \frac{\psi_1^{\ell-1}}{v_1 \Delta t^{\ell}}$$

$$-M_2^{\ell} \psi_1^{\ell} + \left\{-L_2^{\ell} + \frac{1}{v_2 T^{\ell}} \left.\frac{\partial T}{\partial t}\right|_{t=t^{\ell}} + \frac{1}{v_2 \Delta t^{\ell}}\right\} \psi_2^{\ell} = \frac{\psi_2^{\ell-1}}{v_2 \Delta t^{\ell}} \qquad 2.1.20$$

At steady state the equation reduces to the following:

$$L_1 \psi_{10} + M_1 \psi_{20} = 0$$

$$M_2 \psi_{10} + L_2 \psi_{20} = 0 \qquad 2.1.21$$

or

$$\bar{M} \bar{\psi}_0 = 0$$

in matrix form.

Similarly, the adjoint equation may be written as follows:

$$\bar{M}^{+} \bar{\psi}^{+} = 0 \qquad 2.1.22$$

and it can be shown that

$$\bar{M}^{+} = \bar{M}^{T} \qquad 2.1.23$$

The adjoint operator is obtained by transposing the matrix operator of the initial flux solution Ref. 2.5.

2.2 Cross Section Representation

This section summarizes the cross sectional representation that is incorporated into the numerical reactor model. Functional forms were chosen for each cross section parameter as a function of the local moderator density and fuel temperature. (It is noted that feedback is not necessary for scram reactivity calculations. A description of feedback is included in this section for completeness).

The cross section functions were assumed to be separable as follows:

$$\Sigma(\rho,T,B,C) = \Sigma_0(\rho,T) + \Sigma_B(\rho,B) + \Sigma_C(\rho,C) \qquad 2.2.1$$

where Σ signifies a two group cross section

ρ is the moderator density (lb/ft^3)

T is the effective fuel temperature (^oF)

B is the boron concentration (ppm)

C is the fraction of control rod insertion

The uncontrolled (and unborated) reactor cross sections (Σ_0) were least square fit to one of the following functions

1) $\Sigma_0 = a + b\rho + c\sqrt{T} + d\rho\sqrt{T}$ (for Σ_r)

2) $\Sigma_0 = a + b\ell n(\rho + \rho_0)$ (for D_2, Σ_{a_2}, $\nu\Sigma_{f_2}$)

3) $\Sigma_0 = a + b\sqrt{T} + c\ell n(\rho + \rho_0) + d\sqrt{T}\,\ell n(\rho + \rho_0)$ (for D_1, Σ_{a_1}, $\nu\Sigma_{f_1}$)

2.2.2

These functions were chosen due to an observed approximate linear variation of the fast cross sections with $\sqrt{T}$ and due to an approximately logarithmic variation with moderator density for most other cross sections. A nearly linear cross section variation of Σ_r with moderator density was observed and a different function was therefore chosen for this parameter.

The change in the reactor cross sections due to boron concentration $\Sigma_B(\rho,B)$ was assumed to depend only on the moderator density and the boron concentration. The assumed function is as follows:

$$\Sigma_B(\rho,B) = B(a_B + b_B\rho) \qquad 2.2.3$$

where a_B and b_B are constants.

This relation assumes a cross section magnitude which is proportional to the boron concentration and linear with moderator density. The constants a_B and b_B are evaluated at two moderator densities and at some reference boron concentration as follows:

$$a_B = \frac{\Sigma_B(\rho_1, B_{ref})\,\rho_2 - \Sigma_B(\rho_2, B_{ref})\,\rho_1}{(\rho_2 - \rho_1)\,B_{ref}}$$

$$b_B = \frac{\Sigma_B(\rho_2, B_{ref}) - \Sigma_B(\rho_1, B_{ref})}{(\rho_2 - \rho_1)\,B_{ref}}$$

The change in cross section due to control rod insertion is evaluated as follows

$$\Sigma_c(\rho, C) = C\,W_c\,\Sigma_{c_0}(\rho) \qquad 2.2.4$$

where C - is the fraction of control rod insertion.

W_c - is a normalization constant which adjusts the rod worth to measured values (Control-Rod-Weighting Factor)

$\Sigma_{c_0}(\rho)$ - is the reference control rod cross section

The reference control rod cross section, $\Sigma_{c_0}(\rho)$, is specified as a function of local moderator density. The functions employed are as follows:

1) $\Sigma_{c_0}(\rho) = a_c + b_c\,\ell n(\rho + \rho_0)$ (for ΔD_1, $\Delta\Sigma_{a_1}$, ΔD_2, $\Delta\Sigma_{a_2}$, $\Delta\nu\Sigma_{f_2}$)

5) $\Sigma_{c_0}(\rho) = a_c + b_c\rho + C_c\rho^2$ (for $\Delta\Sigma_r$, $\Delta\nu\Sigma_{f_1}$)

2.2.5

2.3 References for Section 2.0

2.1 Ott, K.O., Meneley, D.A., "Accuracy of the Quasistatic Treatment of Spatial Reactor Kinetics" NSE-36, pp. 402-411 (1969).

2.2 Yasinsky, J.B. "Notes on Nuclear Reactor Kinetics" WAPD-TM-1960 (July 1970).

2.3 Menely, D.A., Ott, K.O., Wiener, E.S., "Influence of the Shape-Function Time Derivative on Spatial Kinetics Calculations in Fast Reactors" Trans. Am. Nuc. Soc., Vol. II, No. 1 (June 10-13, 1968).

2.4 Henry, A. [illegible] ation of Parameters Appearing in the Kinetics Equations", [illegible] (December 1955).

2.5 Lamarsh, J.R., "Introduction to Nuclear Reactor Theory" Addison-Wesley (1966).

3.0 FIESTA Computer Code

This section describes the space-time code FIESTA. A general discussion of the solution strategy of the Space-Time Factorization method is presented along with the subroutine structure of the FIESTA code. The FIESTA code is written in FORTRAN and is operational on the CDC-7600 computer. The neutronics model is identical to a previously published model (References 3.1, 3.2 and 3.3).

3.1 Code Structure

The structure of the FIESTA code is presented in figure 3.1, where the function of each subroutine is briefly described in Table 3.1. Figure 3.1 also shows the subroutines which are used only for feedback calculations. These subroutines are not used in scram reactivity calculations, but are presented here for completeness.

3.2 Numerical Solution Strategy

One of the features of the Space-Time-Factorization method is that the Point-Kinetics approximation is simply a special case of the more general method. The Point-Kinetics approximation results if the neutron flux shape changes during a transient may be neglected. The method therefore has the potential of having a rapid numerical solution during those portions of the transient in which flux shape changes are not important.

The space-time factorization method separates variables of the neutron diffusion equation according to their characteristic time constants. The flux amplitude is calculated by the Point-Kinetics equations using very small time steps (the FIESTA code reduces or expands these time steps as needed in order to achieve a converged Point-Kinetics solution). The flux shape is calculated by the shape equation using a time step specified by the user. For the space-time factorization method, a general time differencing numerical scheme can be envisioned wherein three separate types of time steps are used for time-differencing transient equations of the reactor model as shown in figure 3.2.

The flux shape is assumed constant during a time interval ΔT_{SHP}, whereas the feedback solution and the Point Kinetics solution are solved with smaller time steps.

In FIESTA the time step for the flux shape solution is user specified and is equal to the time step for the thermal-hydraulic solution $\Delta T_{SHP} = \Delta T_{TH}$. The time step for the Point Kinetics solution is automatically specified by the code.

The code solution strategy is as follows:

1. It is assumed that $\psi^{\ell-1}$ is constant over the time step ΔT_{SHP}

2. The amplitude equation (Point Kinetics equation) is solved over time step ΔT_{SHP} using estimated variations of the kinetics parameters over the time step ΔT_{SHP} ($\underset{\wedge}{\rho}$ and $\underset{\wedge}{\beta}_i$ are extrapolated forward using a quadratic time dependence from previously known values at time points ℓ-1, ℓ-2 and ℓ-3).

3. The flux shape equation is solved at time point ℓ using new rod position.

4. The kinetics parameters are solved at time point ℓ using the new flux shape.

5. A quadratic fit is performed for the kinetics parameters using new values at time point ℓ and previous time points ℓ-1 and ℓ-2.

6. The amplitude equation is solved again over time step ΔT_{SHP}.

7. The flux shape equation is solved at time point ℓ using rod position and cross section changes due to feedback, where feedback is calculated during the time step using the average power

$$\bar{P}(x) = \frac{P^{\ell}(x) + P^{\ell-1}(x)}{2}$$

8. Steps 4 to 7 are repeated until the amplitude T^{ℓ} is converged.

3.3 References for Section 3.0

3.1 Ferguson, K.L., "Development and Examination of Data Handling Schemes for Reactivity Measurements in the Pressence of Spatial Effects in Large Nuclear Power Reactors". Phd Thesis, Carnegie-Mellon University (1973).

3.2 Eisenhart, L.D., Poncelet, C.G., "Quasistatic Applications to Parabolic Equations with Application to Nuclear Reactor Kinetics", Proc. Int. Symposium on Numerical Solutions of Partial Differential Equations", University of Maryland (1970).

3.3 Decher, U. "Light Water Reactor Accidents: A consistent Analysis of the importance of Space-time Effects" Phd Thesis, Carnegie-Mellon University (1975).

TABLE 3.1

Subroutine Description

1.	FIESTA	main controlling program
2.	INREAD	initializes the problem
3.	REDLIST	namelist input routine
4.	FLXCNT	control of steady state flux solution
5.	PROP	computes the water property table based on the reactor pressure
6.	PINDIPP	calculates fuel pin geometrical factors and relative radial power density in the pin
7.	SETROD	computes position of the control rod tip
8.	CALMAC	calculates reactor cross sections based on control rod location, coolant density, fuel temperature and boron concentration
9.	RODFD	control rod cross section calculation based on the local water density
10.	COEF	computes coefficients of the steady state finite differenced flux equations
11.	GUESS	provides an initial guess of the fast and thermal flux equations
12.	INTEG	a generalized spatial integration routine
13	FLXSWP	fast and thermal flux calculation
14.	POWER1	spatial power calculation
15.	FEEDBK	steady state TWIGL feedback equations
	FEEDBK2	steady state thermo-hydraulic calculation with detailed fuel pin thermal model and two phase flow analysis
16.	DENS	water density calculation for subcooled liquid
17.	DNB3	W-3 DNBR correlation
	DNB4	Janssen Levy DNBR correlation
18.	FILM	coolant film coefficient calculation

TABLE 3.1 (Continued)

19.	FUNT	water temperature calculation from enthalpy
20.	PINHEAT	calculates the coefficients of the tridiagonal matrix for the steady state and for the transient heat transfer within the fuel rod.
21.	PROPTH	UO_2 and Zirconium heat transfer properties
22.	GAP	computes the clad-pellet gap conductance
23.	TRIDA	tri-diagonal matrix solution
24.	AVTEMPF	computes average fuel temperature
25.	PICK,POCK	fuel temperature retrieval and storage routines
26.	SUBVOID	coolant void model for two phase flow
27.	ADJCNT	controls the adjoint flux solution
28.	ADJSWP	solves for the adjoint flux
29.	PARA	solves the kinetics parameters ρ, β, Λ and performs the initial normalization of the neutron amplitude function
30.	DIFFUSE	integrates the spatial neutron diffusion operator
31.	OUTEDT	writes all output results
32.	PTOEDT	reduces all $\nu\Sigma_f$ cross sections by the steady state eigenvalue
33.	RHOEDIT	detailed reactivity edit
34.	DELTK	spatial k_∞ edit
35.	DRIVER	controls the transient solution
36.	INDLNT	computes the initial precursor concentrations
37.	PRINTO	controls output print
38.	INTERPO	computes inlet enthalpy, reactor pressure, boron concentration, and inlet flow based on input tables; also calculates enthalpy mixing in the plenum, and computes the inlet enthalpy for the time-delay flow model
39.	MOVROD	computes control rod tip position from control rod velocity equation

TABLE 3.1 (Continued)

40.	PITKIN	Point-Kinetics calculation
41.	THTR	transient TWIGL feedback equations
	THTR2	transient thermo-hydraulic calculation with detailed fuel pin thermal model and two-phase flow
42.	DELAY	time dependent delayed neutron precursor calculation
43.	WEIGHT	spatial weighting coefficient calculation
44.	TRCOEF	computes coefficients of the transient finite differenced flux equations
45.	SOLVE	computes transients neutron flux shape

FIGURE 3.1

FIESTA Subroutine Structure

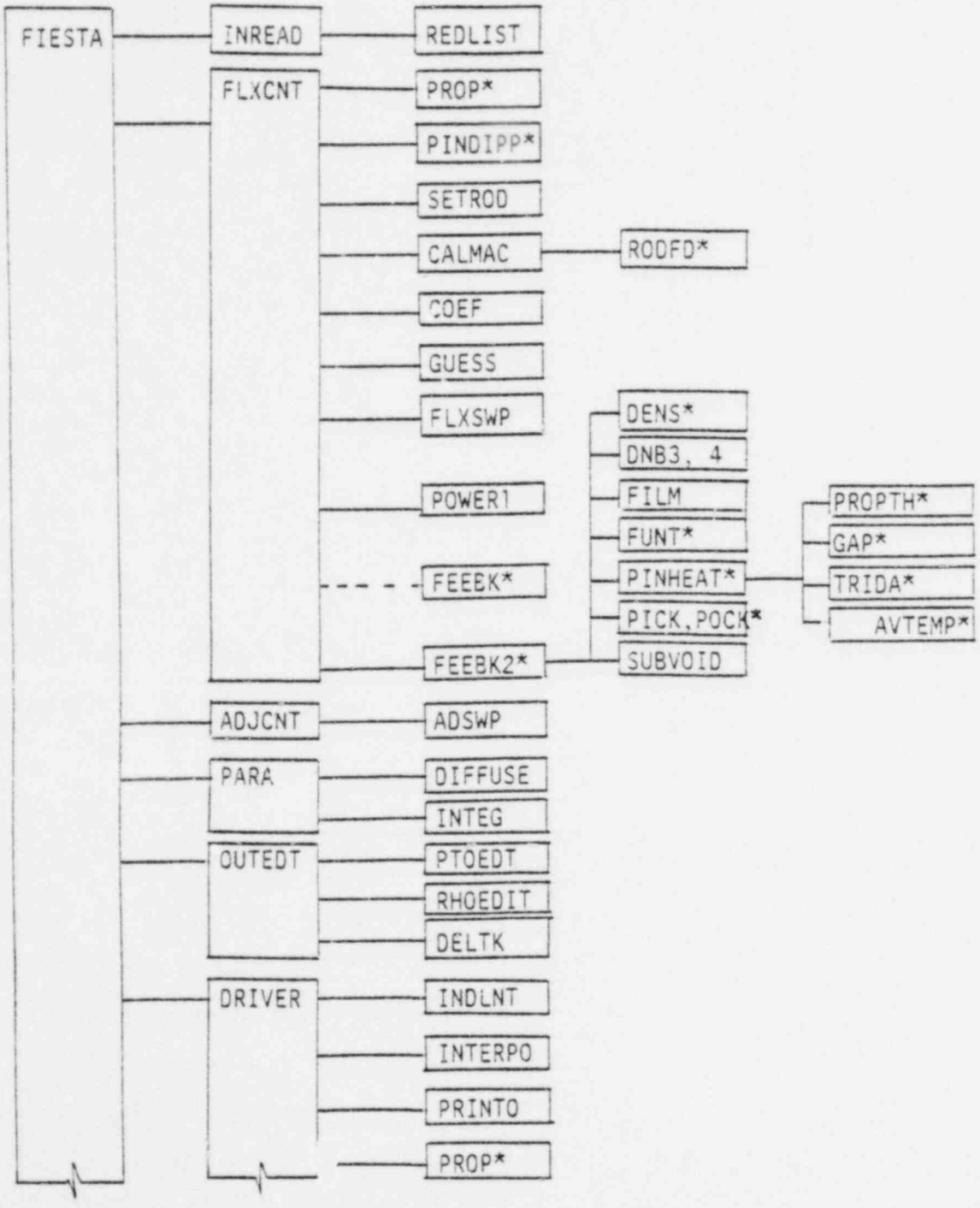

(*These subroutines are needed only for feedback calculations)

FIGURE 3.1 (Continued)

FIESTA Subroutine Structure

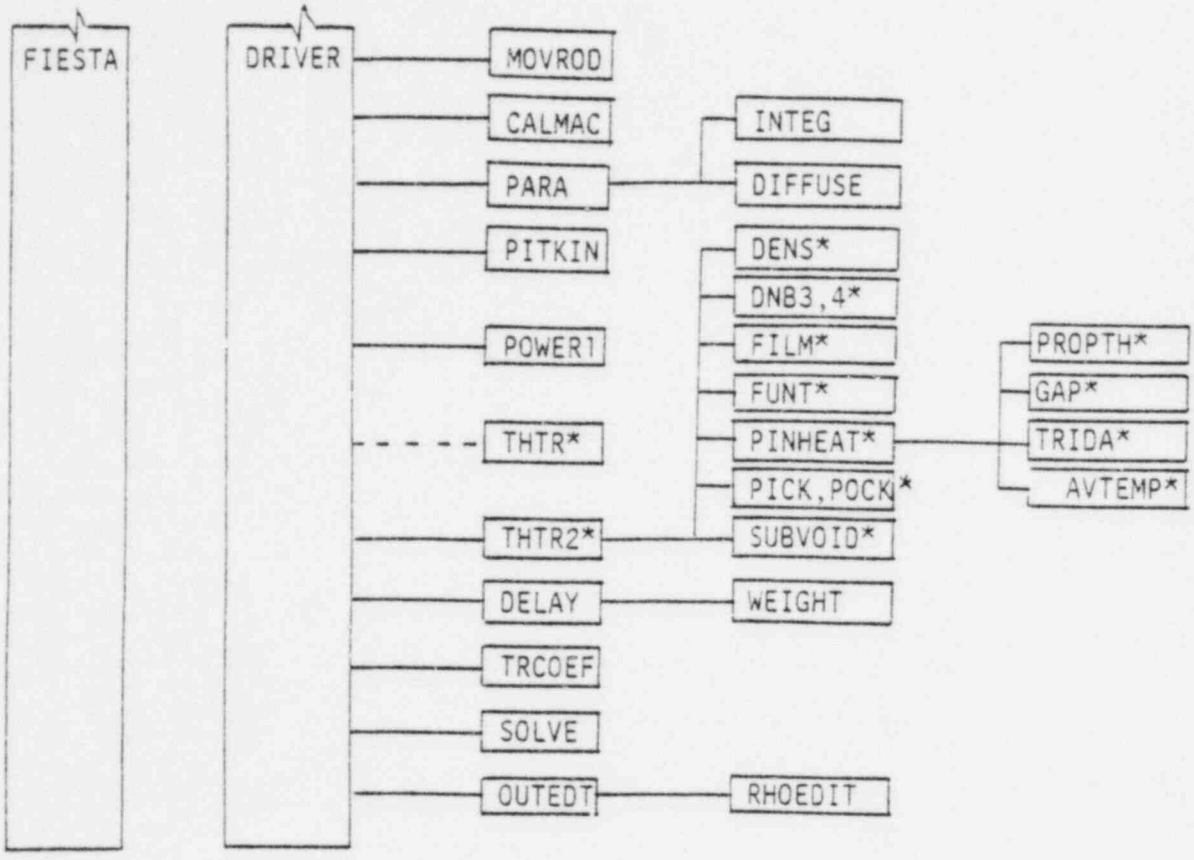

(*These subroutines are needed only for feedback ca'culations)

FIGURE 3.2

General Time Differencing Model

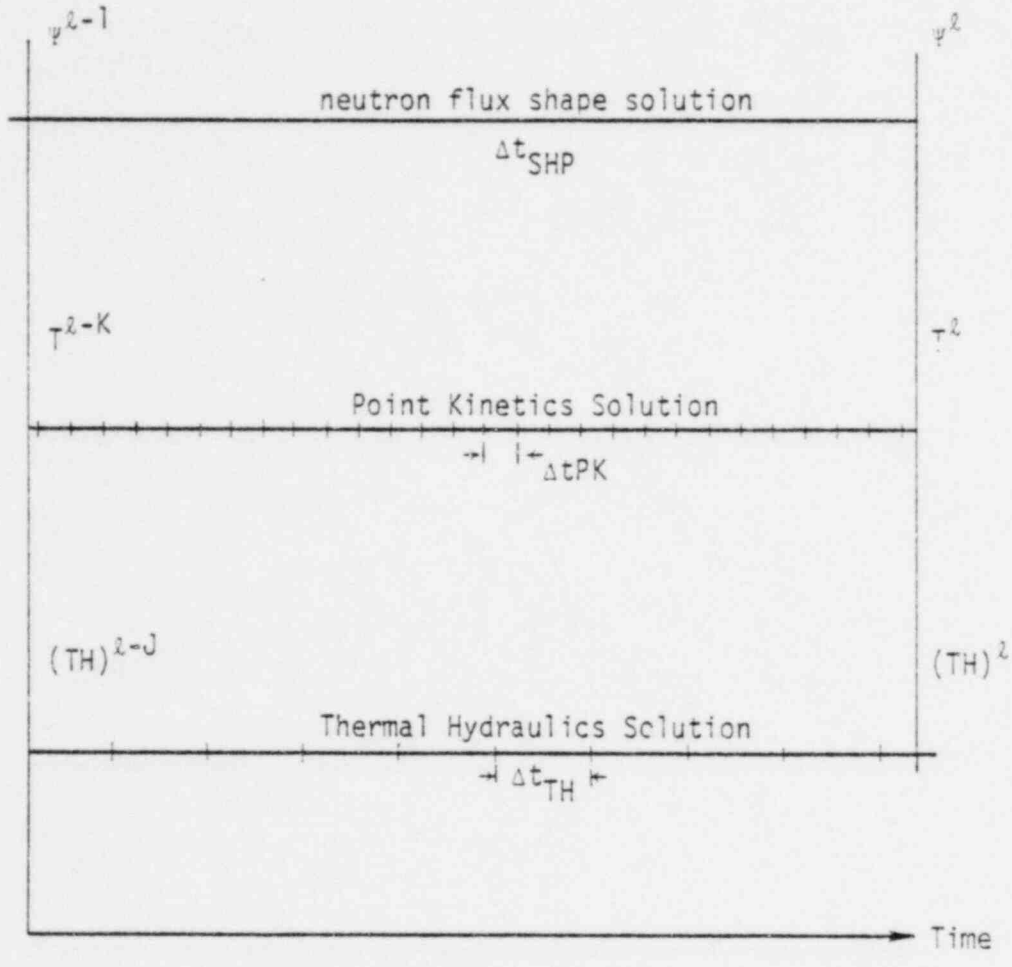

4.0 Verification of the FIESTA Code

The FIESTA code has been verified by comparison with several benchmark problems discussed in Reference 4.1, and by comparison with HERMITE (Ref. 4.2). Results of these comparisons are presented in this section.

4.1 Comparisons with Benchmark Problem

This section describes the results of the benchmark problem comparisons.

The benchmark problems described in reference 4.1 consist of an infinite slab reactor model with three regions as shown in figure 4.1.

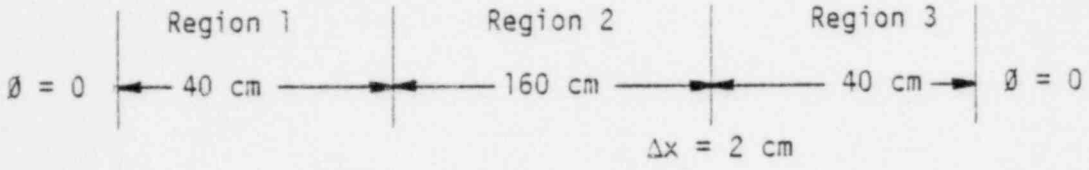

Figure 4.1

Infinite Slab Reactor Model

Cross sections and delayed neutron parameters are presented in Table 4.1.

4.1.1 Subcritical Transient

For the subcritical transient, the thermal absorption cross section, Σ_a^2, in region 1 is linearly increased by 3% in one second. Results are shown in table 4.2 for various codes.

Table 4.2 shows that FIESTA agrees well with other codes, eventhough the mesh structure had to be altered slightly in FIESTA due to a mesh limitation in FIESTA.

Table 4.3 shows the kinetics parameters that are calculated by FIESTA for this transient. These kinetics parameters are not usually available in other space-time codes therefore no comparison is possible.

The kinetics parameters are shown in equations 2.1.19.

It is noted that $\beta(t) = \beta$ a constant, since the function F(t) has been chosen to be an integral over the fission cross section, so that it is identical to the numerator of the integral defining β.

The flux amplitude is also shown in Table 4.3. This flux amplitude is the solution to the Point Kinetics equations. It is nearly equal to the power (Table 4.2).

The reactor power may be written as follows:

$$\frac{P(t)}{Po} = \frac{\langle \Sigma_f(r,E,t)\ \Psi(r,E,t)\rangle}{\langle \Sigma_{fo}(r,E)\ \Psi_o(r,E)\rangle}\ T(t) \qquad 4.1.1$$

Since the neutron flux shape is normalized such that

$$\langle \Psi_o^+(r,E)\ \frac{1}{v(E)}\ \Psi(r,E,t)\rangle = \text{constant}$$

a good agreement between power, and flux amplitude is expected whenever the space-energy distribution of $\frac{\Psi^+}{v}$ closely approximates the space-energy distribution of Σ_f or when the flux shape change is small.

4.1.2 Supercritical Transient

The second benchmark problem consists of a supercritical transient using the same initial problem goemetry. A supercritical transient is induced by linearly decreasing the regional thermal absorption cross section by 1% in one second. Results of the code comparison are shown in Table 4.4.

The kinetics parameters computed by FIESTA are shown in Table 4.5.

4.2 FIESTA-HERMITE comparisons.

In order to verify the FIESTA code for the specific use of calculating scram reactivities an additional comparison was performed between FIESTA and HERMITE.

The problem analyzed consisted of an axial reactor scram, in which control rods are inserted linearly into the core in 3.0 seconds. Results are shown in Figure 4.2 for the power comparisons. The power shape comparison during the transient are shown in figures 4.3 through figures 4.8.

The excellent agreement between FIESTA and HERMITE verifies FIESTA for calculating scram reactivities.

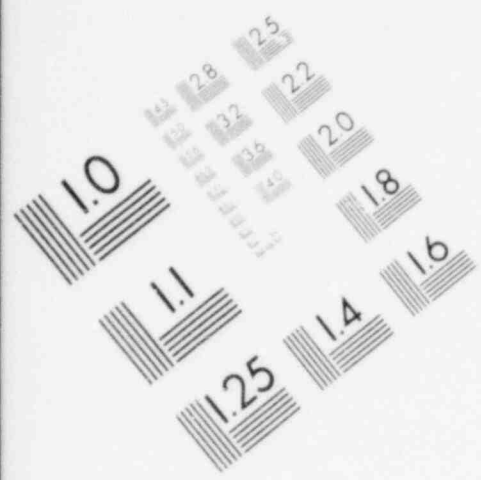

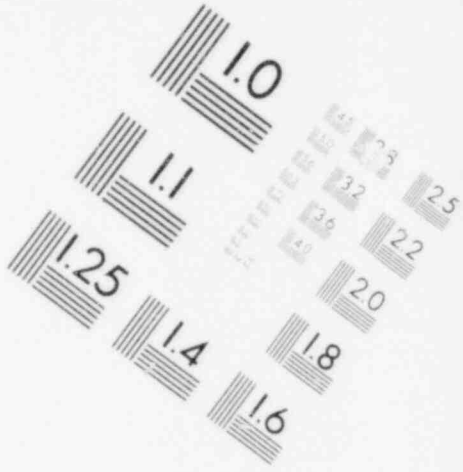

IMAGE EVALUATION
TEST TARGET (MT-3)

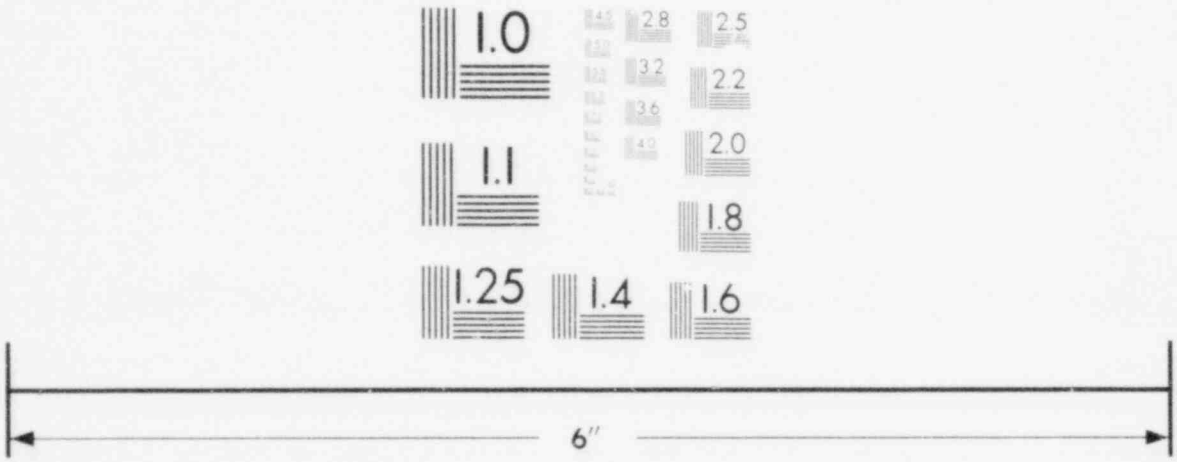

MICROCOPY RESOLUTION TEST CHART

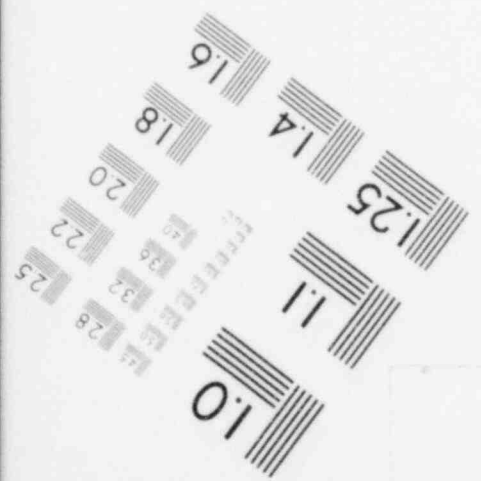

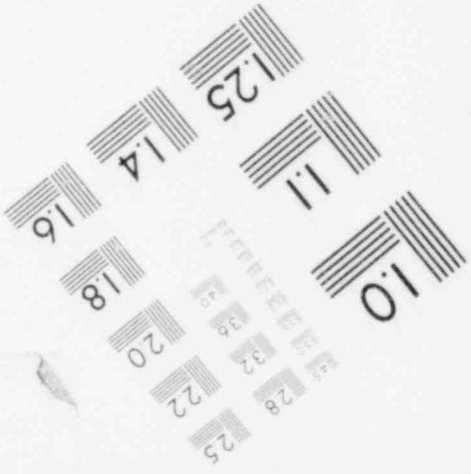

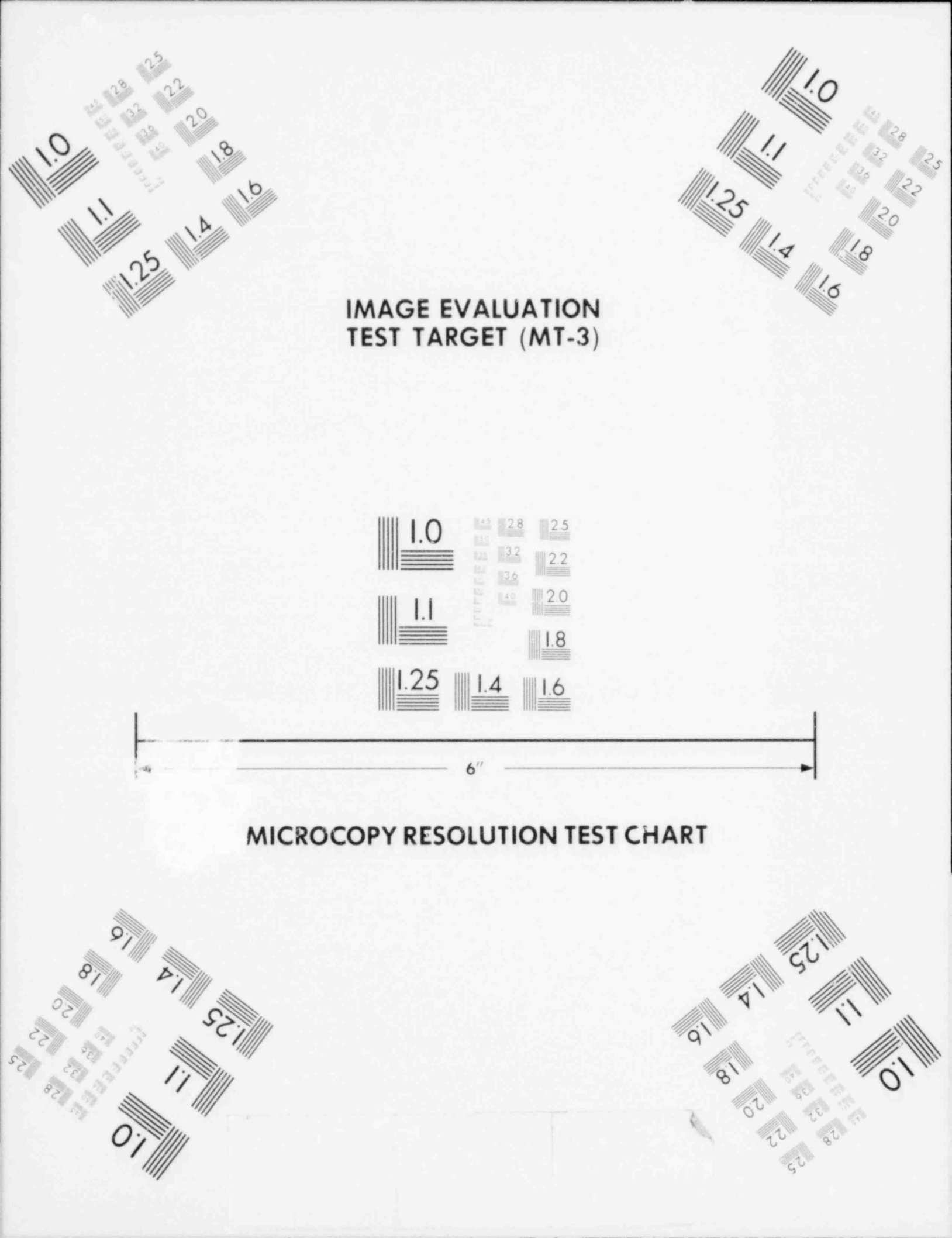
IMAGE EVALUATION
TEST TARGET (MT-3)
1.0
1.1
1.25
1.4
1.6
1.8
2.0
2.2
2.5
2.8
3.2
3.6
4.0
4.5
6"
MICROCOPY RESOLUTION TEST CHART

4.3 References For Section 4.0

4.1 "Argonne Code Center: Numerical Determination of the Space-Time, angle or energy distribution of particles in an assembly" ANL-7416 supplement 1, December 1972.

4.2 CENPD-188, "HERMITE-A 3-D Space-Time Neutronics Code with Thermal Feedback".

TABLE 4.1

Cross Section and Delayed Neutron Parameters for the Benchmark Problems

	Region			Region	
	1 and 3	2		1 and 3	2
D^1 (cm)	1.50	1.00	$\Sigma^{1\to2}$ (cm^{-1})	.015	.010
D^2 (cm)	.50	.50	χ^1	1.00	1.00
Σ_a^1 (cm^{-1})[a]	.026	.02	χ^2	0	0
Σ_a^2 (cm^{-1})[a]	.18	.08	v^1 (cm/sec)	1.0×10^7	1.0×10^7
$v\Sigma_f^1$ (cm^{-1})	.010	.005	v^2 (cm/sec)	3.0×10^5	3.0×10^5
$v\Sigma_f^2$ (cm^{-1})	.200	.099			

[a]Total removal cross section, including Σ_c, Σ_f, and $\Sigma^{1\to2}$.

Additional Data

Delayed Neutron Parameters

Type	Effective Delay Fraction	Decay Constant (sec^{-1})	Type	Effective Delay Fraction	Decay Constant (sec^{-1})
1	.00025	.0124	4	.00296	.3010
2	.00164	.0305	5	.00086	1.1400
3	.00147	.1110	6	.00032	3.0100

TABLE 4.2

Subcritical Benchmark Problem Results

Code	RAUMZEIT (4.1)	WIGLE (4.1)	QX1 (4.1)	HERMITE (4.2)	FIESTA
k_{eff}	.9015507	.9015507	.9015507	.9015162	.9015473
			Power/Initial Power		
t=0 seconds	1.0	1.0	1.0	1.0	1.0
.1	.9299	.9298	.9298	.9296	.9295
.2	.8733	.8732	.8733	.8732	.8730
.5	.7597	.7596	.7597	.7598	.7595
1.0	.6588	.6588	.6588	.6590	.6587
1.5	.6432	.6432	.6433	.6434	.6431
2.0	.6307	.6306	.6307	.6309	.6306
number of mesh intervals	120	120	120	120	96*
ΔX	2 cm	2 cm	2 cm	2 cm	36 @ 2 cm 24 @ 4 cm 36 @ 2 cm

*FIESTA is currently limited to 100 mesh intervals.

TABLE 4.3

Kinetics Parameters for the
Subcritical Benchmark Problem

(FIESTA Results)

Time (seconds)	Reactivity ρ	Delayed Neutron Fraction β	Prompt Neutron Lifetime (10^{-4} sec)	Flux Amplitude T
0	$.6538 \times 10^{-8}$*	$.75 \times 10^{-2}$	.21299	1.0
.1	$-.0580 \times 10^{-2}$	$.75 \times 10^{-2}$	.21324	.92928
.2	$-.10788 \times 10^{-2}$	$.75 \times 10^{-2}$	.21345	.87265
.5	$-.22009 \times 10^{-2}$	$.75 \times 10^{-2}$	.21394	.75885
1.0	$-.32797 \times 10^{-2}$	$.75 \times 10^{-2}$	.21441	.65784
1.5	$-.31476 \times 10^{-2}$	$.75 \times 10^{-2}$	.21436	.64235
2.0	$-.30414 \times 10^{-2}$	$.75 \times 10^{-2}$	.21432	.62983

* ρ_0 is a measure of the convergence to a critical solution.

TABLE 4.4

Supercritical Benchmark
Problem Results

Code	(Ref. 4.1) RAUMZEIT	(Ref. 4.1) WIGLE	(Ref. 4.1) QX1	(Ref. 4.2) HERMITE	FIESTA
k_{eff}	.9015507	.9015507	.9015507	.9015162	.9015473
			Power/Initial Power		
t=0 seconds	1.0	1.0	1.0	1.0	1.0
.1	1.028	1.028	1.028	1.029	1.029
.2	1.063	1.062	1.063	1.063	1.063
.5	1.205	1.205	1.205	1.204	1.206
1.0	1.740	1.740	1.740	1.738	1.741
1.5	1.959	1.959	1.959	1.955	1.959
2.0	2.166	2.165	2.166	2.159	2.165
3.0	2.606	2.605	2.606	NA	2.604
4.0	3.108	3.107	3.108	NA	3.106

TABLE 4.5

Kinetics Parameters for the
Supercritical Benchmark Problem
(FIESTA Results)

Time (seconds)	Reactivity ρ	Delayed Neutron Fraction β	Prompt Neutron Lifetime (10^{-4} sec)	Flux Amplitude T
0	$.6538 \times 10^{-8}$*	$.75 \times 10^{-2}$	.21299	1.0
.1	$.02141 \times 10^{-2}$	$.75 \times 10^{-2}$	.21289	1.0289
.2	$.04403 \times 10^{-2}$	$.75 \times 10^{-2}$	.21280	1.0631
.5	$.12084 \times 10^{-2}$	$.75 \times 10^{-2}$	.21247	1.2058
1.0	$.29050 \times 10^{-2}$	$.75 \times 10^{-2}$	.21173	1.7426
1.5	$.30054 \times 10^{-2}$	$.75 \times 10^{-2}$	.21168	1.9608
2.0	$.30801 \times 10^{-2}$	$.75 \times 10^{-2}$	.21164	2.1674
3.0	$.3198 \times 10^{-2}$	$.75 \times 10^{-2}$	.21158	2.6073
4.0	$.32870 \times 10^{-2}$	$.75 \times 10^{-2}$	.21153	3.1097

*ρ_0 is a measure of the convergence to a critical solution.

Figure 4.2

COMPARISON OF FIESTA AND HERMITE POWER DURING A REACTOR SCRAM
(6% $\Delta\rho$ TOTAL ROD WORTH)

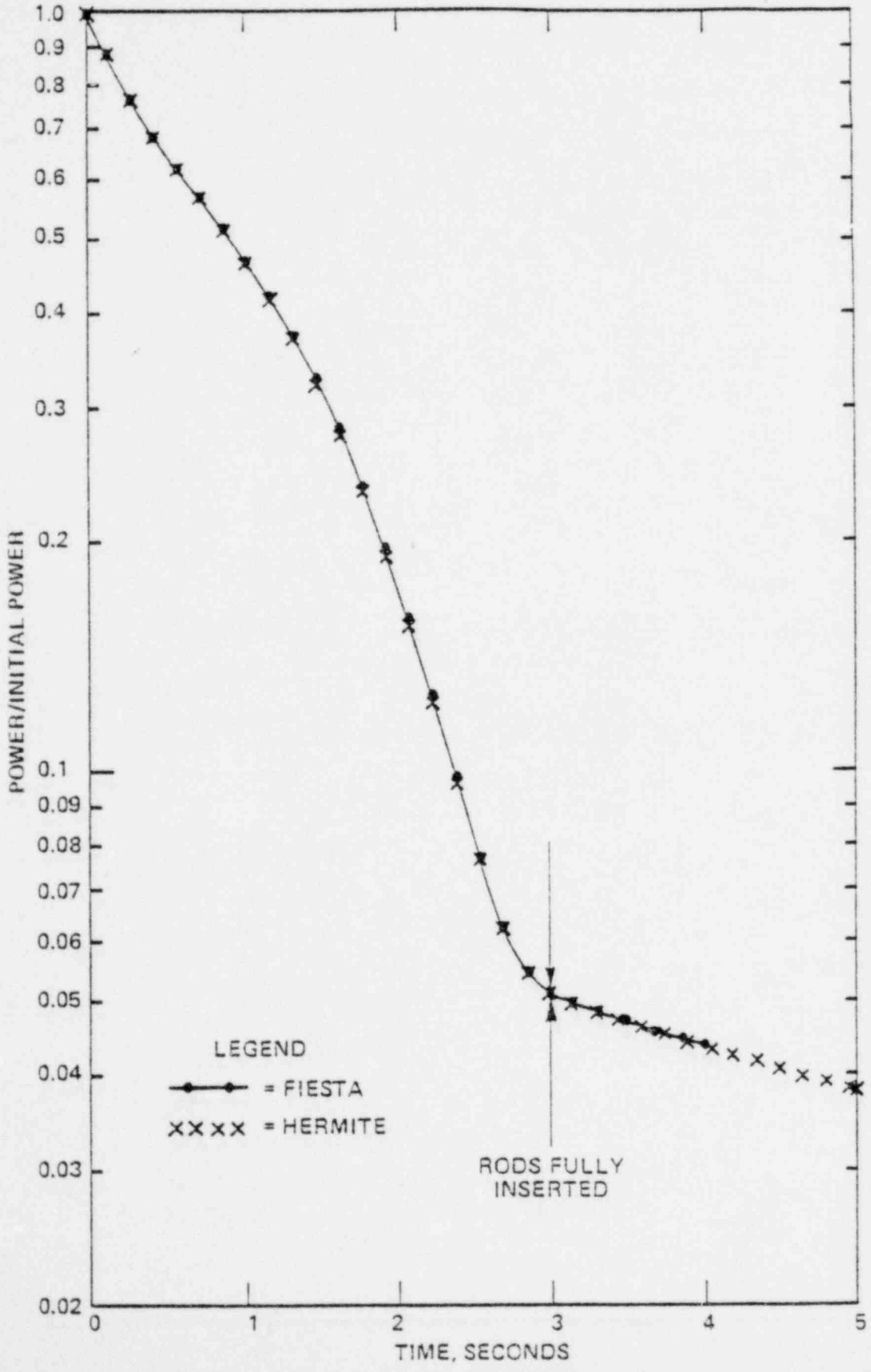

Figure 4.3

COMPARISON OF THE FIESTA AND HERMITE POWER SHAPE DURING A REACTOR SCRAM
(CORE HEIGHT = 136.7 IN) INITIAL POWER SHAPE (ARO)
TIME = 0 SECONDS

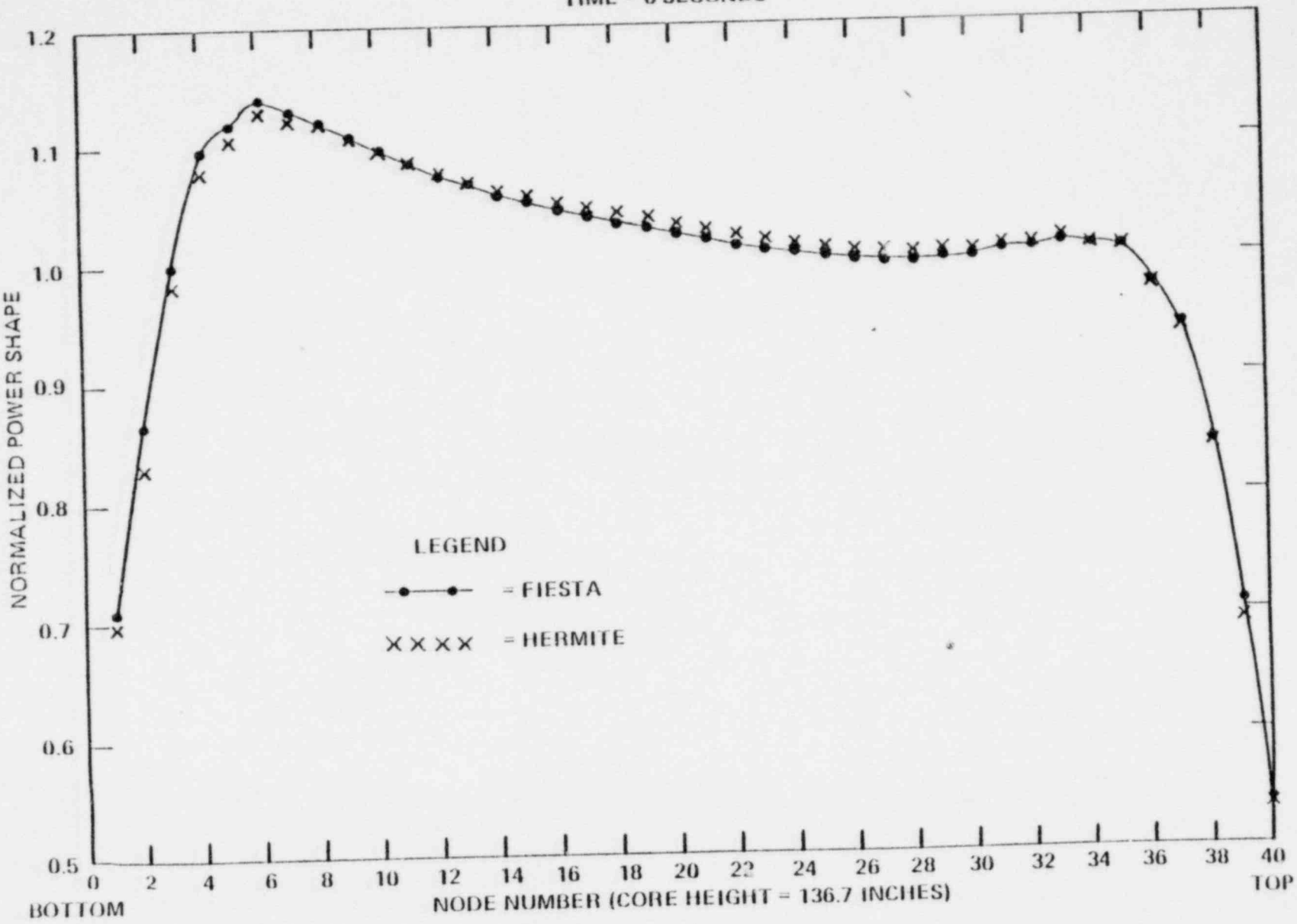

Figure 4.4

COMPARISON OF THE FIESTA AND HERMITE POWER SHAPE DURING A REACTOR SCRAM
(CORE HEIGHT = 136.7 IN) POWER SHAPE AT 20% ROD INSERTION
TIME = 0.6 SECONDS

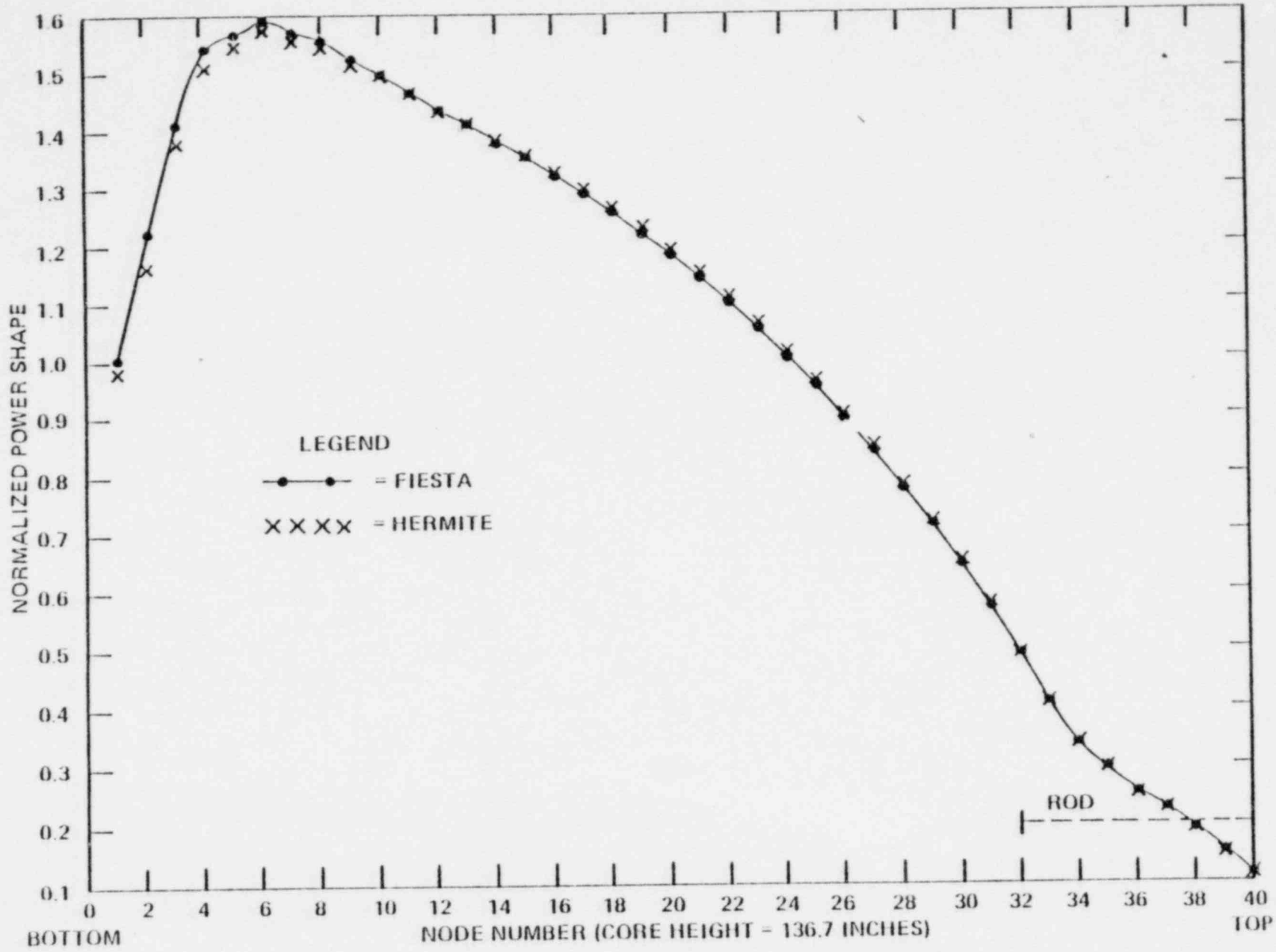

Figure 4.5

COMPARISON OF THE FIESTA AND HERMITE POWER SHAPE DURING A REACTOR SCRAM
(CORE HEIGHT = 136.7 IN) POWER SHAPE AT 40% ROD INSERTION
TIME = 1.2 SECONDS

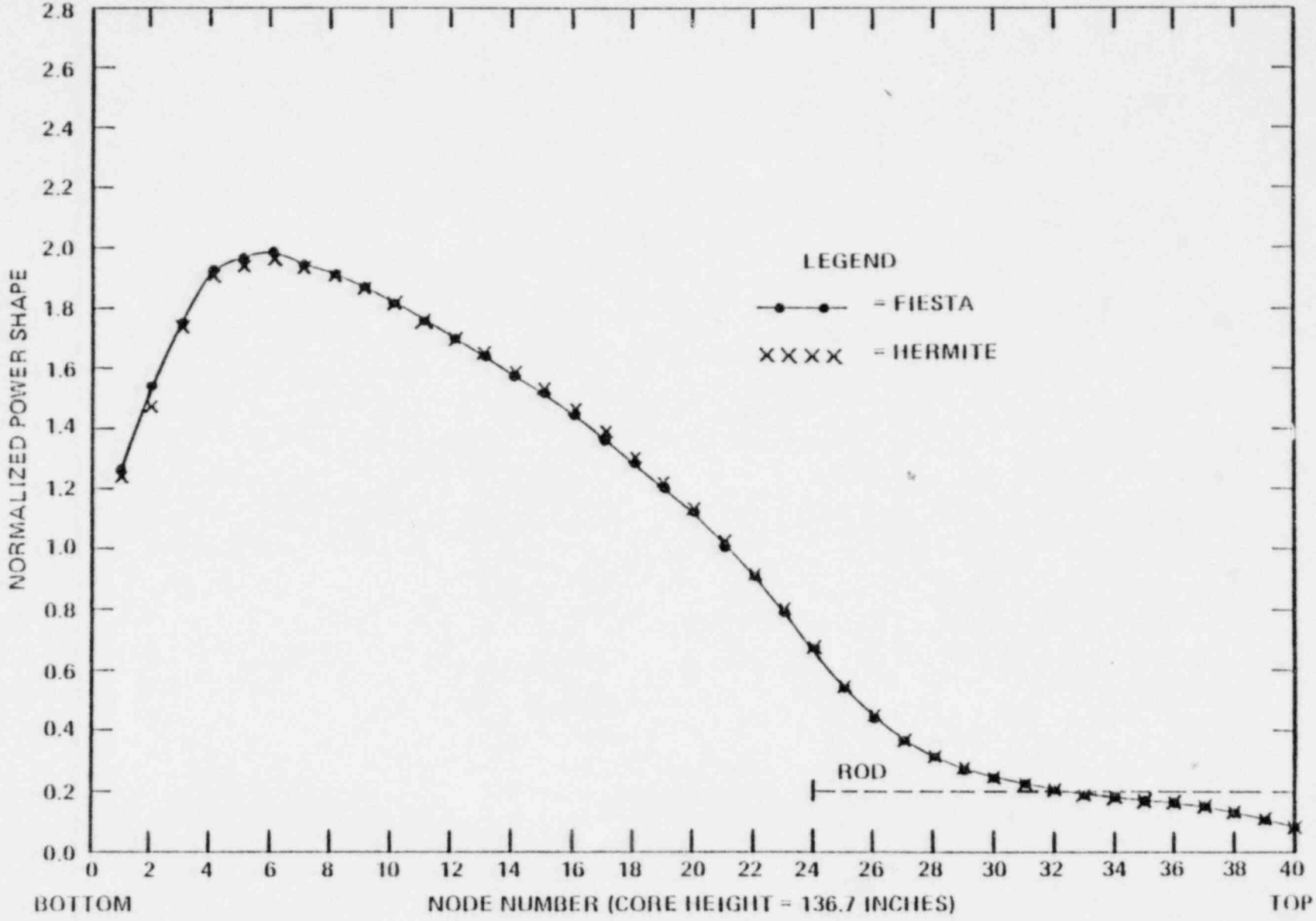

Figure 4.6

COMPARISON OF THE FIESTA AND HERMITE POWER SHAPE DURING A REACTOR SCRAM
(CORE HEIGHT = 136.7 IN) POWER SHAPE AT 60% ROD INSERTION
TIME = 1.8 SECONDS

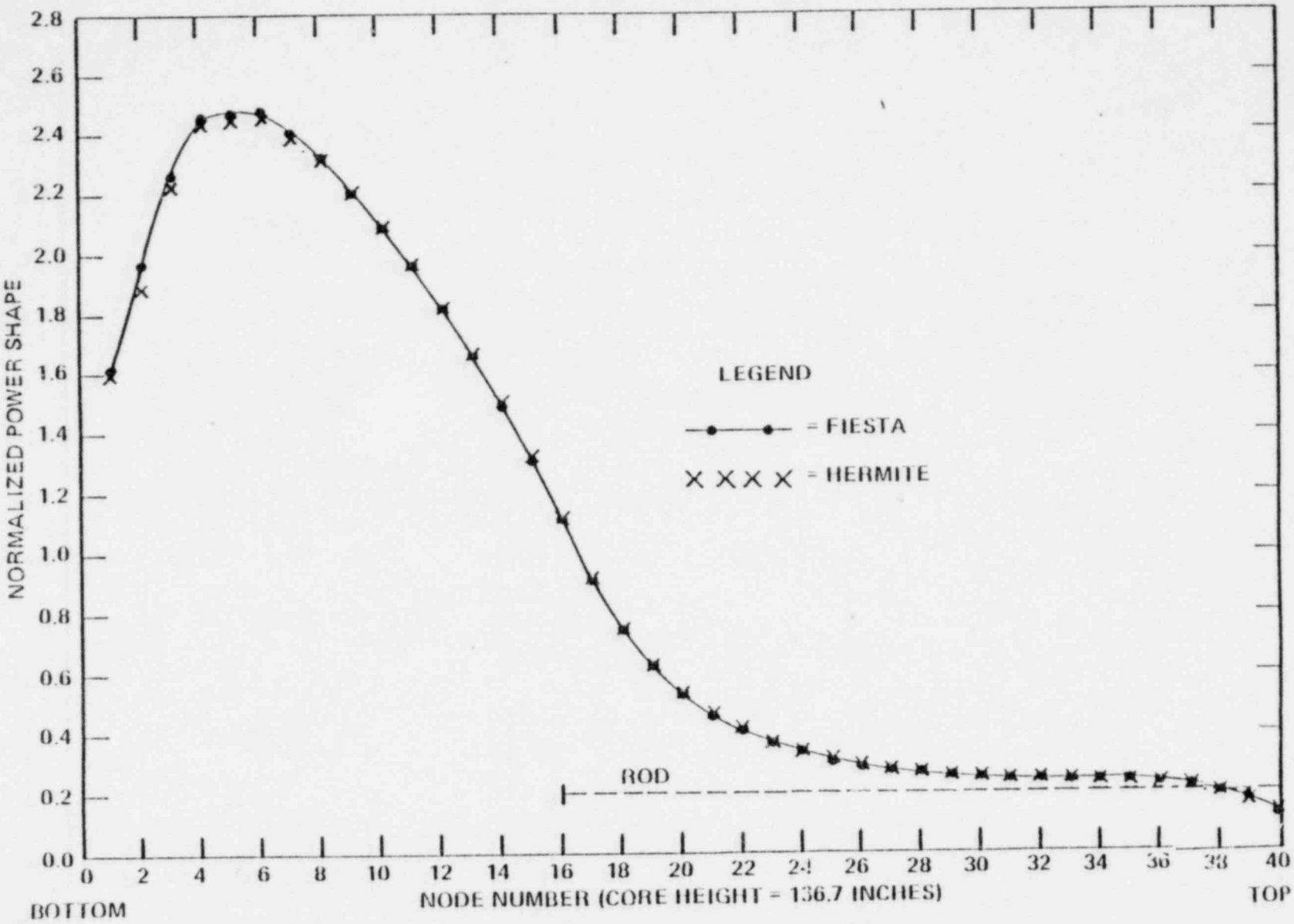

Figure 4.7

COMPARISON OF THE FIESTA AND HERMITE POWER SHAPE DURING A REACTOR SCRAM

(CORE HEIGHT = 136.7 IN) POWER SHAPE AT 80% ROD INSERTION

TIME = 2.4 SECONDS

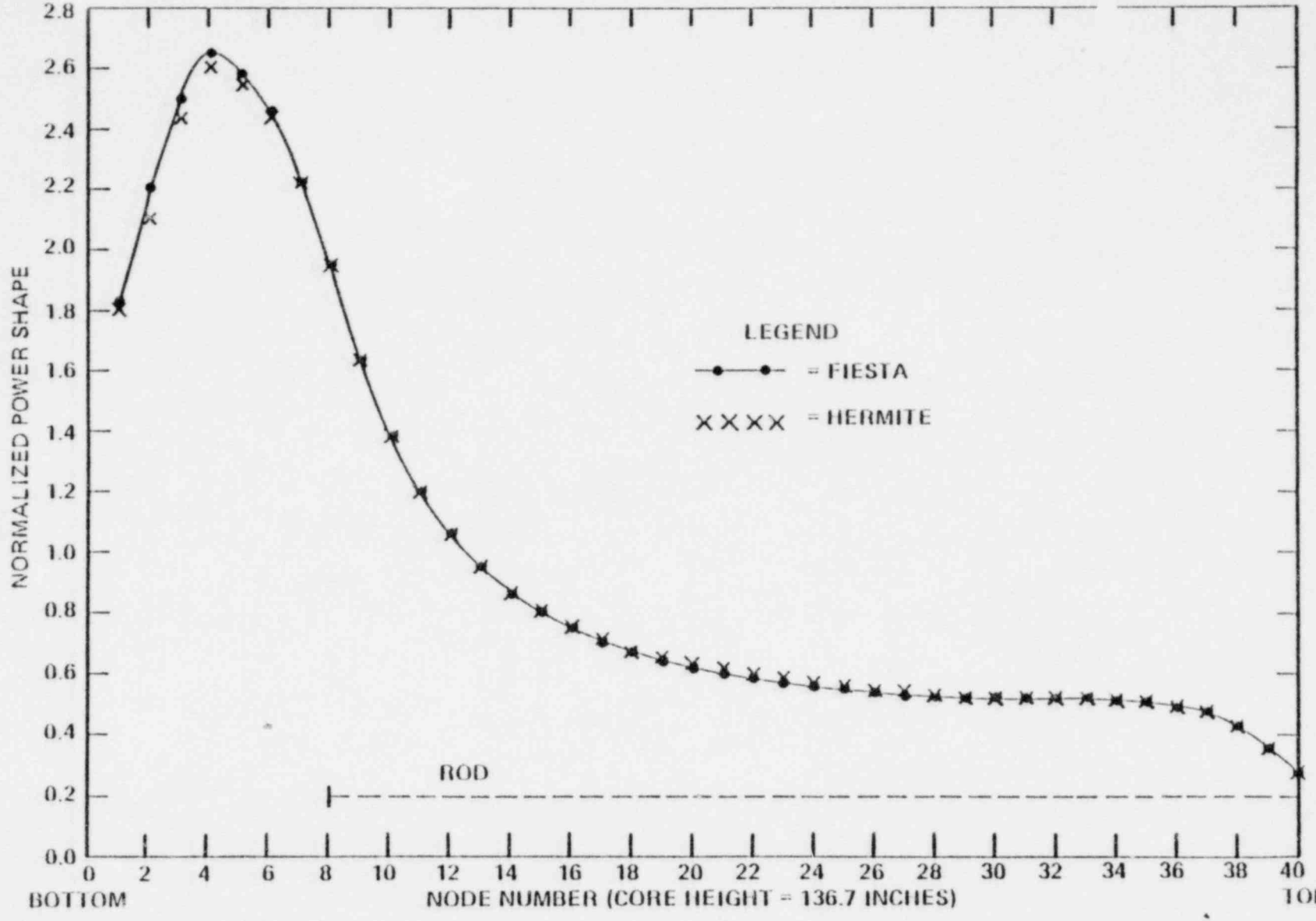

Figure 4.8

COMPARISON OF THE FIESTA AND HERMITE POWER SHAPE DURING A REACTOR SCRAM
(CORE HEIGHT = 136.7 IN) POWER SHAPE AT 100% ROD INSERTION
TIME = 3.0 SECONDS

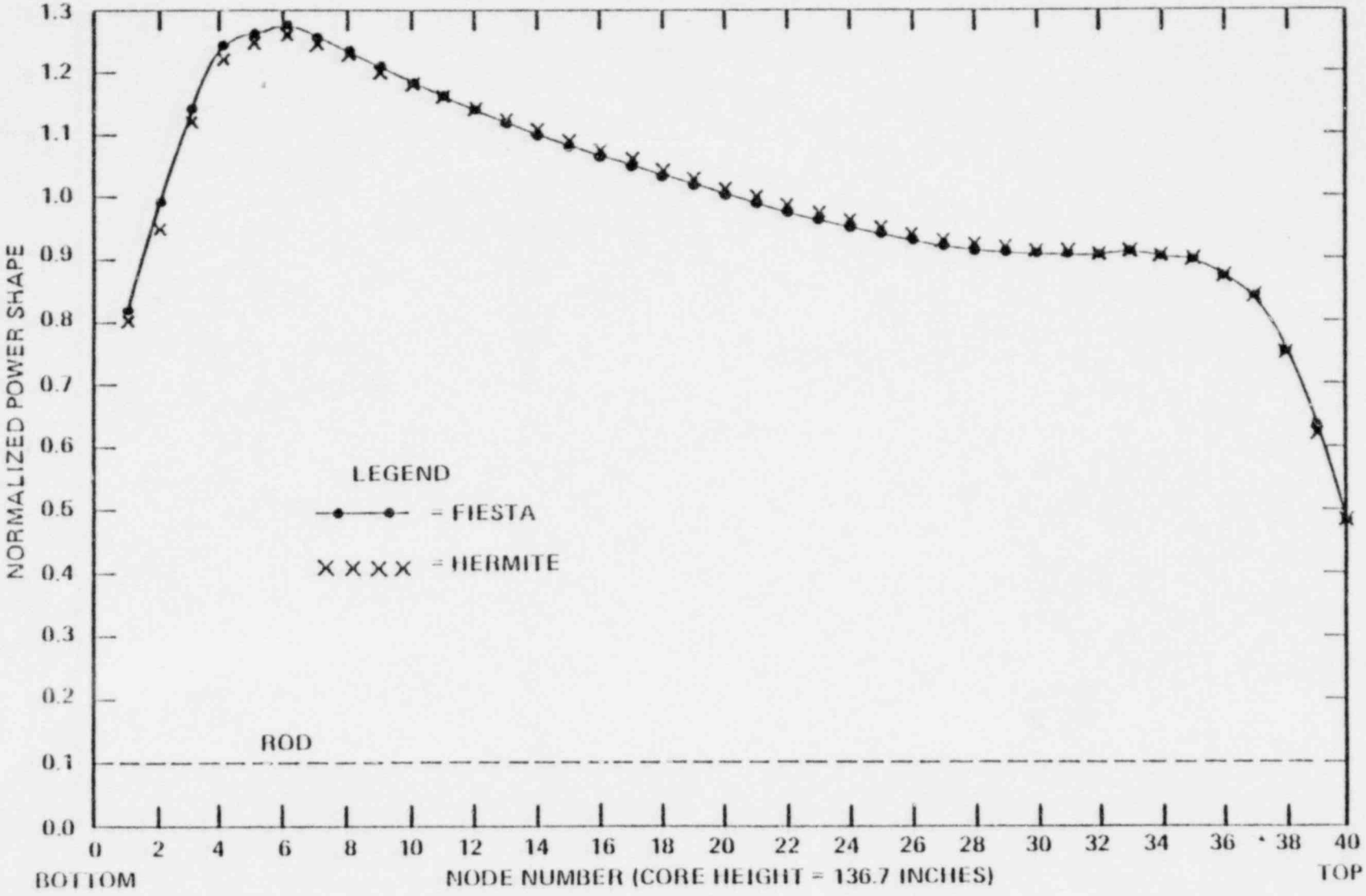

5.0 Space-Time Results

This section presents typical results for a space-time scram reactivity analysis. The first section (5.1) presents scram reactitivities for a typical cycle, using space-time d ition of reactivity, and compares them to the static reactivity ition. The second section (5.2) discusses the impact of using t pace-time definition of scram reactivities on the results of analyses of design basis transients.

5.1 Space-Time and Static Scram Reactivity Comparisons

Space-time calculations more accurately predict the axial flux shape during a rod insertion than do critical static calculations. The reason for this difference is that space-time calculations account for the presence of delayed neutron precursors, which are neglected in static calculations. The delayed neutron precursors reduce the axial tilt away from the rods, compared to static calculations, and hence increase the negative reactivity which is inserted during a scram. This effect is largest during the early portion of the scram and is nearly nonexistent at full rod insertion when both definitions of reactivity agree. Figures 5.1 and 5.2 show the results for two different initial power shapes. These figures show that at intermediate rod insertions space-time negative reactivity insertions due to rods can be much l rger than the predicted static reactivities.

The reactivities used in the safety analysis are based on a large number of calculations such as those shown in Figures 5.3 through 5.6. These figures show the scram reactivities as a function of the initial power shape (ASI). Typical results are shown for both static and space-time definitions of reactivity. The lower bounds of these calculations which envelope the scram reactivities as a function of initial ASI are used in safety analyses. These lower bound reactivities are shown in Table 5.1 for a case with 6% $\Delta\rho$ total rod worth.

In order to calculate the scram reactivity for a total rod worth other than 6% $\Delta\rho$, correction factors are developed. Scram reactivities are calculated at off nominal reactivities (such as 2, 4, 8 and 10%$\Delta\rho$) to calculate reactivity ratios relative to the base case (base 6%). These reactivity ratios are shown in Figures 5.7 through 5.10 for the example given. Lower bound values of these calculated ratios are used to calculate scram reactivity ratios shown in Table 5.2 The values presented in Tables 5.1 and 5.2 define the negative space-time reactivity insertion as a function of initial ASI, rod insertion and total rod worth.

5.2 Benefits of Space-Time Reactivities

The benefit of using Space-Time versus quasi-static calculated scram reactivities is the insertion of a larger amount of negative reactivity at a given CEA position. The added reactivity will slow down the core power rise and result in a lower peak power. Also, the additional scram reactivity will cause both the core power and the core average heat flux to decrease at a faster rate following the initiation of the scram. The net result is to lower peak powers and heat fluxes and hence reduce the margin requirements (i.e., a gain in operating flexibility). This is true for all Design Bases Events (DBE's) where a trip is initiated.

As an example of the benefits of using Space-Time reactivities versus the quasi-static scram reactivities, one can consider the Loss of Flow transient. For the 4-pump Loss of Flow DBE, the reduction in the margin requirement is typically 1 to 3% when calculated using the standard CESEC-TORC methodology.

TABLE 5.1

Reactivity insertion (%Δρ) during a scram from all rods out, for a 6%Δρ rod worth for various axial shape indices(ASI) (reactivities computed by space time methods) core height = 136.7 inches

PCT INSERTION	ASI -.6	-.4	-.2	0.0	+.2	+.4	+.6
5	.19	.14	.10	.07	.03	.01	.002
10	.47	.35	.25	.14	.07	.02	.0045
15	.79	.62	.4	.21	.10	.04	.0075
20	1.15	.80	.5	.27	.13	.05	.012
25	1.60	1.07	.65	.33	.16	.06	.02
30	2.14	1.37	.80	.41	.19	.08	.03
35	2.70	1.72	1.0	.5	.23	.10	.043
40	3.50	2.14	1.17	.59	.27	.13	.07
45	4.25	2.50	1.37	.7	.33	.18	.10
50	4.82	2.95	1.62	.81	.4	.24	.15
55	5.25	3.35	1.95	1.0	.52	.34	.24
60	5.42	3.90	2.33	1.22	.68	.48	.37
65	5.50	4.35	2.75	1.51	.85	.66	.57
70	5.68	4.77	3.27	1.91	1.15	.93	.85
75	5.75	5.15	3.85	2.50	1.75	1.38	1.25
80	5.80	5.47	4.47	3.24	2.55	2.07	1.95
85	5.89	5.73	5.13	4.10	3.55	3.09	2.95
90	5.89	5.89	5.57	5.07	4.70	4.47	4.25
95	5.94	5.94	5.87	5.77	5.61	5.55	5.3
100	6.0	6.0	6.0	6.0	6.0	6.0	6.0

TABLE 5.2

Ratio of the reactivity inserted during a scram at various rod positions relative to the reactivity inserted for a 6%Δρ total rod worth scram from ARO core height 136.7 inches space time method

5% rod insertion

Total rod worth %Δρ	ASI -.6	-.4	-.2	0	.2	.4	.6
10	1.40	1.38	1.36	1.34	1.32	1.33	1.42
8	1.20	1.20	1.19	1.17	1.16	1.20	1.40
4	.69	.70	.71	.72	.73	.72	.71
2	.38	.39	.41	.42	.41	.40	.38

10% rod insertion

	ASI -.6	-.4	-.2	0	.2	.4	.6
10	1.30	1.26	1.23	1.20	1.18	1.19	1.30
8	1.15	1.14	1.12	1.10	1.09	1.12	1.19
4	.75	.78	.80	.81	.80	.80	.78
2	.45	.47	.49	.52	.54	.52	.48

15% rod insertion

	ASI -.6	-.4	-.2	0	.2	.4	.6
10	1.25	1.22	1.17	1.14	1.12	1.14	1.25
8	1.14	1.12	1.11	1.06	1.05	1.07	1.17
4	.76	.81	.83	.85	.86	.85	.79
2	.46	.51	.55	.59	.61	.59	.52

20% rod insertion

	ASI -.6	-.4	-.2	0	.2	.4	.6
10	1.25	1.20	1.15	1.11	1.10	1.12	1.22
8	1.13	1.12	1.08	1.06	1.05	1.07	1.15
4	.76	.81	.85	.86	.86	.85	.81
2	.47	.53	.57	.61	.61	.61	.55

TABLE 5.2 (Continued)

25% rod insertion

Total rod worth %Δρ	ASI -.6	-.4	-.2	0	.2	.4	.6
10	1.27	1.20	1.13	1.11	1.09	1.11	1.19
8	1.13	1.12	1.06	1.05	1.04	1.05	1.13
4	.74	.80	.83	.87	.87	.86	.79
2	.45	.51	.58	.63	.67	.62	.52

30% rod insertion

	ASI -.6	-.4	-.2	0	.2	.4	.6
10	1.28	1.22	1.14	1.10	1.08	1.11	1.19
8	1.16	1.12	1.08	1.05	1.03	1.05	1.15
4	.75	.80	.83	.87	.87	.86	.75
2	.44	.51	.56	.64	.65	.63	.54

35% rod insertion

	ASI -.6	-.4	-.2	0	.2	.4	.6
10	1.36	1.24	1.15	1.11	1.11	1.12	1.19
8	1.19	1.12	1.07	1.04	1.04	1.05	1.1
4	.69	.80	.85	.88	.89	.85	.80
2	.39	.49	.56	.61	.67	.62	.50

40% rod insertion

	ASI -.6	-.4	-.2	0	.2	.4	.6
10	1.41	1.27	1.17	1.11	1.10	1.12	1.19
8	1.20	1.13	1.07	1.05	1.05	1.06	1.12
4	.69	.76	.80	.85	.87	.84	.78
2	.38	.46	.54	.60	.65	.61	.51

TABLE 5.2 (Continued)

45% rod insertion

Total rod worth %Δρ	ASI -.6	-.4	-.2	0	.2	.4	.6
10	1.50	1.30	1.21	1.12	1.12	1.13	1.23
8	1.24	1.15	1.09	1.04	1.04	1.05	1.12
4	.67	.72	.78	.84	.85	.84	.78
2	.35	.43	.51	.61	.63	.60	.48

50% rod insertion

	ASI -.6	-.4	-.2	0	.2	.4	.6
10	1.52	1.34	1.23	1.15	1.15	1.15	1.21
8	1.25	1.15	1.10	1.07	1.06	1.07	1.10
4	.66	.72	.78	.83	.84	.83	.80
2	.33	.43	.50	.57	.62	.58	.50

55% rod insertion

	ASI -.6	-.4	-.2	0	.2	.4	.6
10	1.55	1.37	1.26	1.17	1.15	1.14	1.17
8	1.27	1.22	1.13	1.08	1.07	1.07	1.10
4	.65	.69	.75	.81	.80	.82	.77
2	.30	.38	.48	.54	.57	.62	.57

60% rod insertion

	ASI -.6	-.4	-.2	0	.2	.4	.6
10	1.60	1.45	1.30	1.18	1.14	1.17	1.20
8	1.28	1.25	1.15	1.08	1.07	1.09	1.12
4	.65	.68	.73	.80	.82	.81	.78
2	.32	.34	.39	.52	.58	.55	.50

TABLE 5.2 (Continued)

65% rod insertion (space-time method)

Total rod worth %Δρ	ASI -.6	-.4	-.2	0	.2	.4	.6
10	1.62	1.51	1.35	1.21	1.18	1.17	1.23
8	1.30	1.26	1.17	1.11	1.09	1.09	1.12
4	.65	.67	.71	.77	.75	.75	.77
2	.32	.33	.40	.5	.52	.51	.47

70% rod insertion

	ASI -.6	-.4	-.2	0	.2	.4	.6
10	1.66	1.56	1.42	1.27	1.21	1.2	1.25
8	1.30	1.28	1.21	1.10	1.08	1.11	1.14
4	.63	.65	.68	.72	.77	.76	.72
2	.33	.33	.37	.44	.48	.48	.47

75% rod insertion

	ASI -.6	-.4	-.2	0	.2	.4	.6
10	1.64	1.60	1.48	1.33	1.26	1.23	1.26
8	1.30	1.28	1.23	1.15	1.12	1.12	1.15
4	.64	.65	.67	.72	.73	.73	.72
2	.3	.32	.34	.42	.46	.47	.46

80% rod insertion

	ASI -.6	-.4	-.2	0	.2	.4	.6
10	1.65	1.61	1.54	1.43	1.38	1.38	1.38
8	1.3	1.31	1.27	1.21	1.20	1.20	1.20
4	.64	.62	.64	.66	.68	.70	.72
2	.30	.315	.33	.36	.40	.43	.40

TABLE 5.2 (Continued)

85% rod insertion (space-time method)

Total rod worth %Δρ	ASI -.6	-.4	-.2	0	.2	.4	.6
10	1.65	1.64	1.60	1.5[illegible]	1.46	1.43	1.43
8	1.30	1.31	1.29	1.25	1.22	1.21	1.4
4	.63	.65	.65	.68	.68	.7	.7
2	.31	.32	.32	.34	.36	.36	.35

90% rod insertion

	ASI -.6	-.4	-.2	0	.2	.4	.6
10	1.65	1.65	1.64	1.61	1.59	1.56	1.55
8	1.3	1.3	1.3	1.3	1.28	1.27	1.26
4	.65	.66	.66	.67	.67	.67	.68
2	.30	.32	.32	.33	.30	.33	.35

95% rod insertion

	ASI -.6	-.4	-.2	0	.2	.4	.6
10	1.65	1.65	1.65	1.65	1.64	1.64	1.64
8	1.33	1.31	1.30	1.30	1.30	1.30	1.30
4	.65	.65	.65	.65	.65	.65	.65
2	.32	.32	.32	.32	.32	.32	.32

100% rod insertion

	ASI -.6	-.4	-.2	0	.2	.4	.6
10	1.66	1.66	1.66	1.66	1.66	1.66	1.66
8	1.33	1.33	1.33	1.33	1.33	1.33	1.33
4	.66	.66	.66	.66	.66	.66	.66
2	.33	.33	.33	.33	.33	.33	.33

Figure 5.1

REACTIVITY INSERTION vs ROD INSERTION FOR A SCRAM FROM ALL RODS OUT (ARO)
USING STATIC AND SPACE-TIME METHODOLOGY

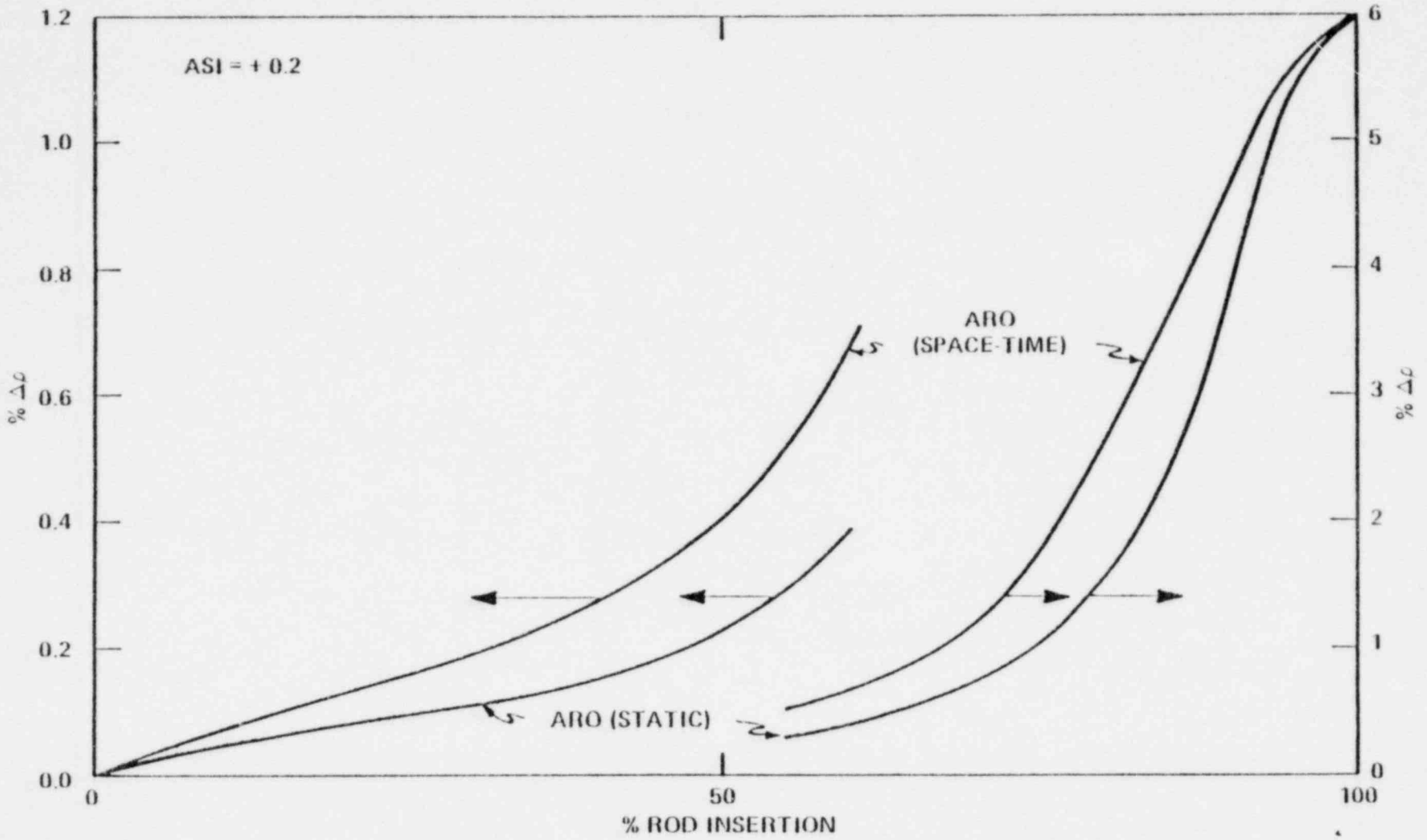

Figure 5.2

REACTIVITY INSERTION vs ROD INSERTION FOR A SCRAM FROM ALL RODS OUT (ARO)
USING STATIC AND SPACE-TIME METHODOLOGY

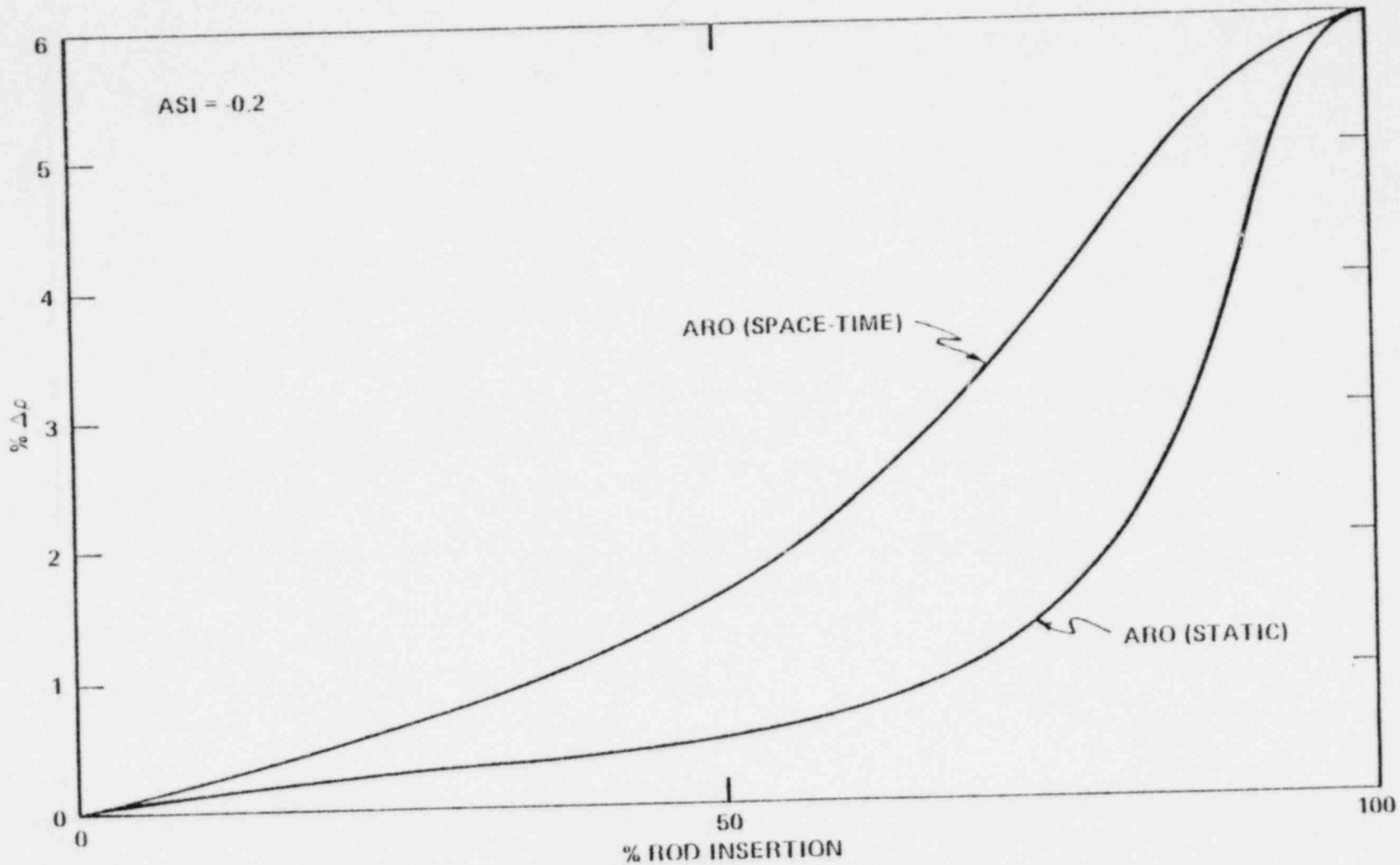

Figure 5.3

SPACE-TIME AND STATIC REACTIVITY COMPARISONS FOR A SCRAM FROM ARO
(20% ROD INSERTION)

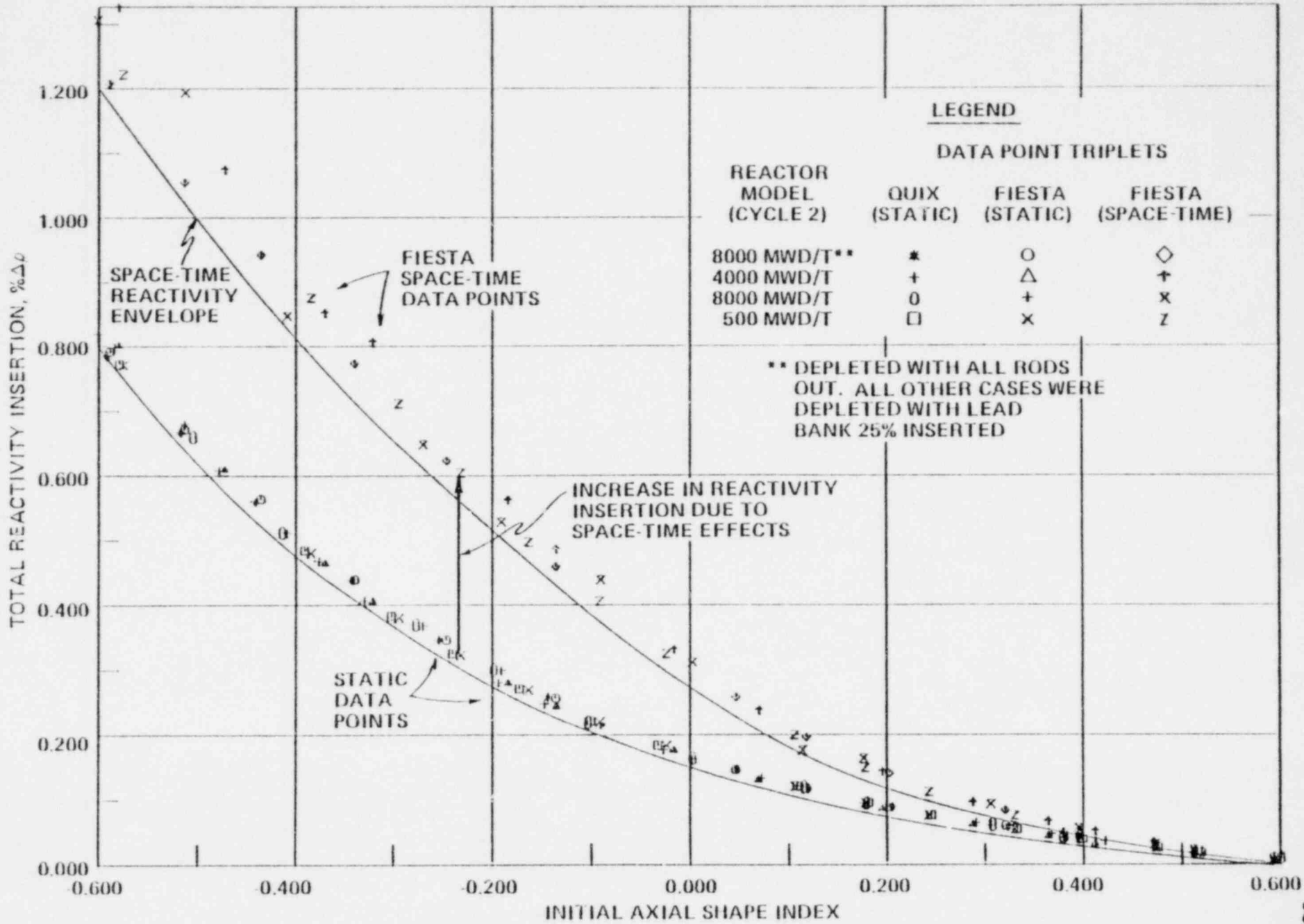

Figure 5.4

SPACE-TIME AND STATIC REACTIVITY COMPARISONS FOR A SCRAM FROM ARO

(40% ROD INSERTION)

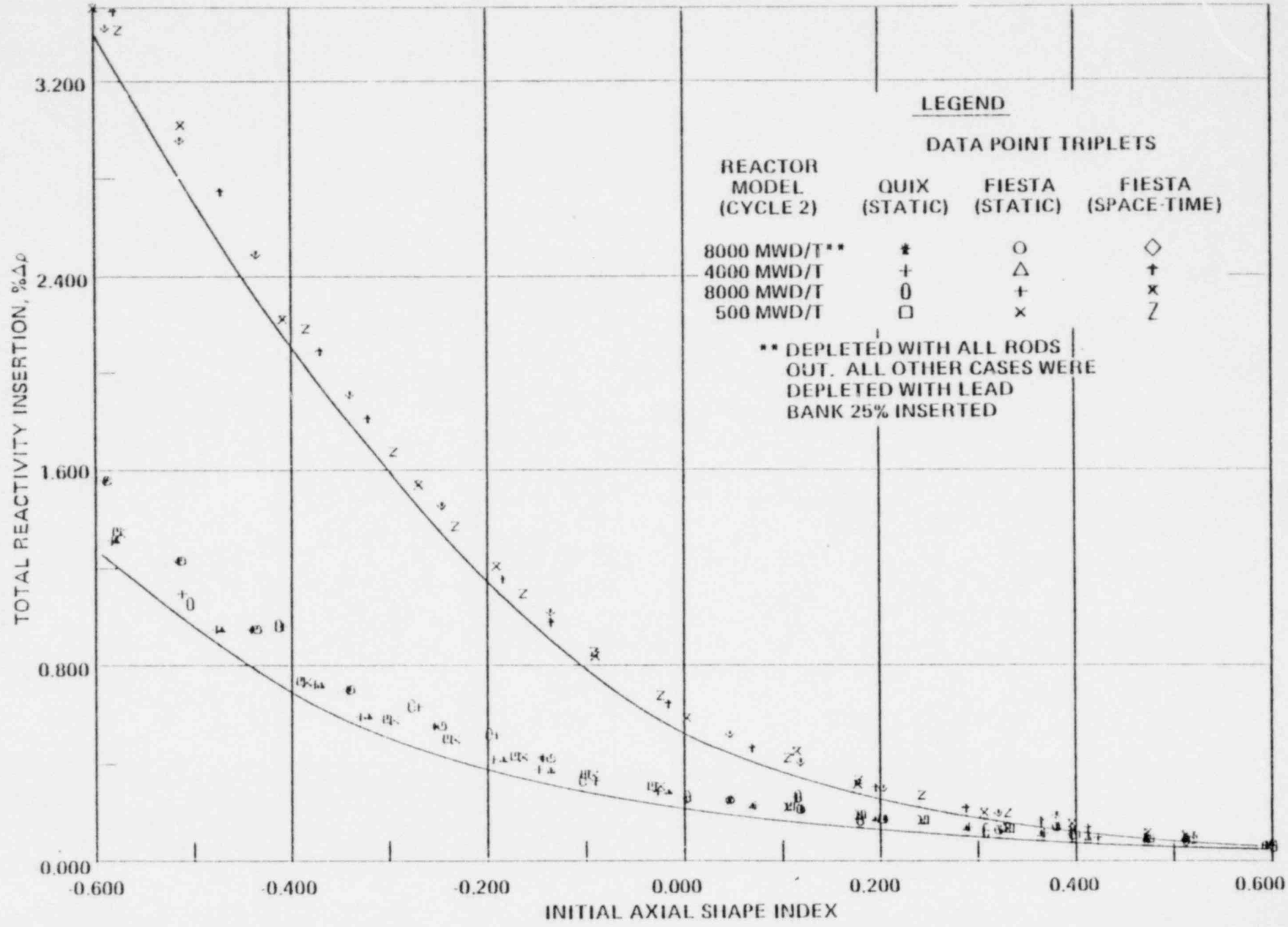

Figure 5.5

SPACE-TIME AND STATIC REACTIVITY COMPARISONS FOR A SCRAM FROM ARO
(60% ROD INSERTION)

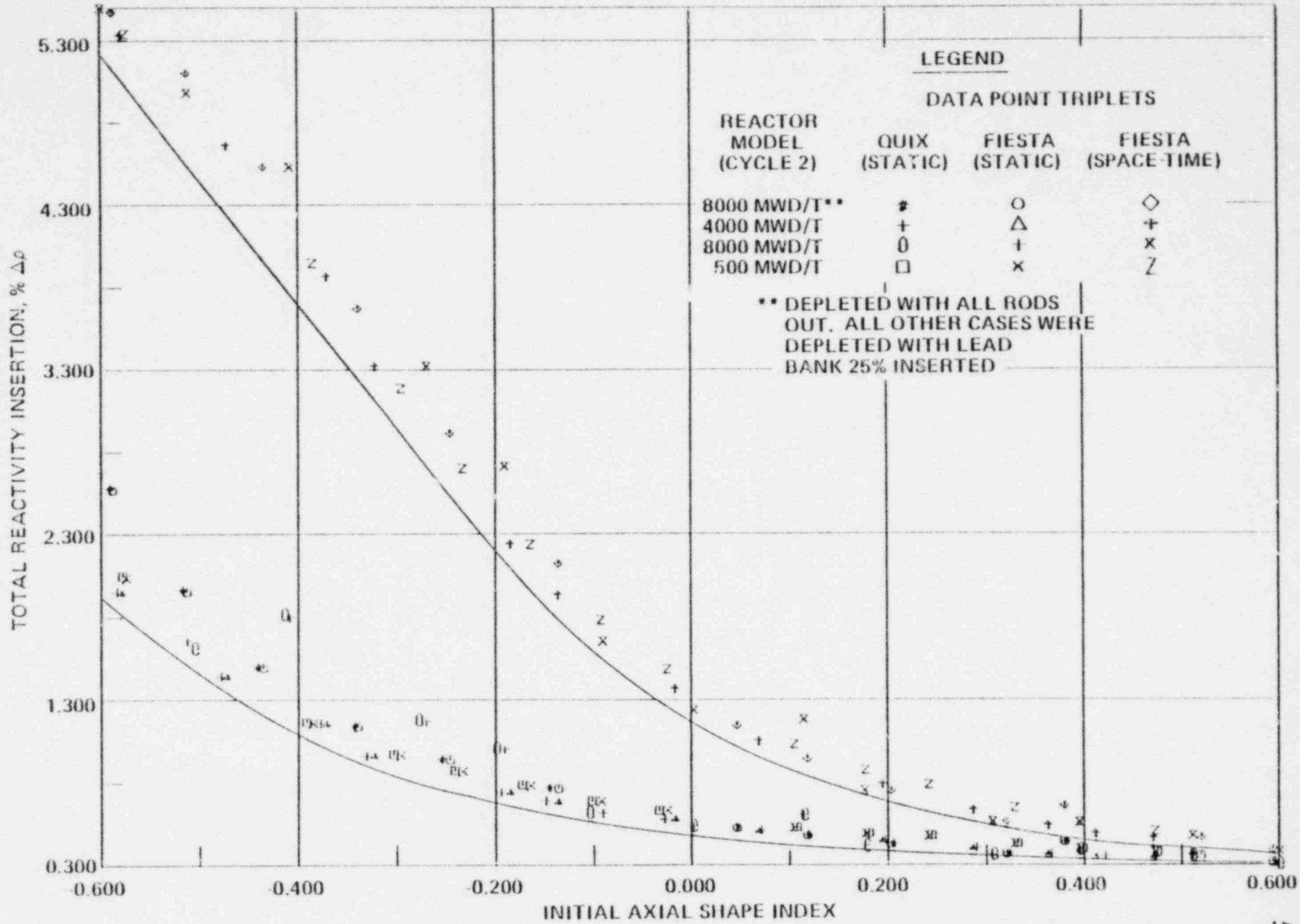

Figure 5.6

SPACE-TIME AND STATIC REACTIVITY COMPARISONS FOR A SCRAM FROM ARO

(80% ROD INSERTION)

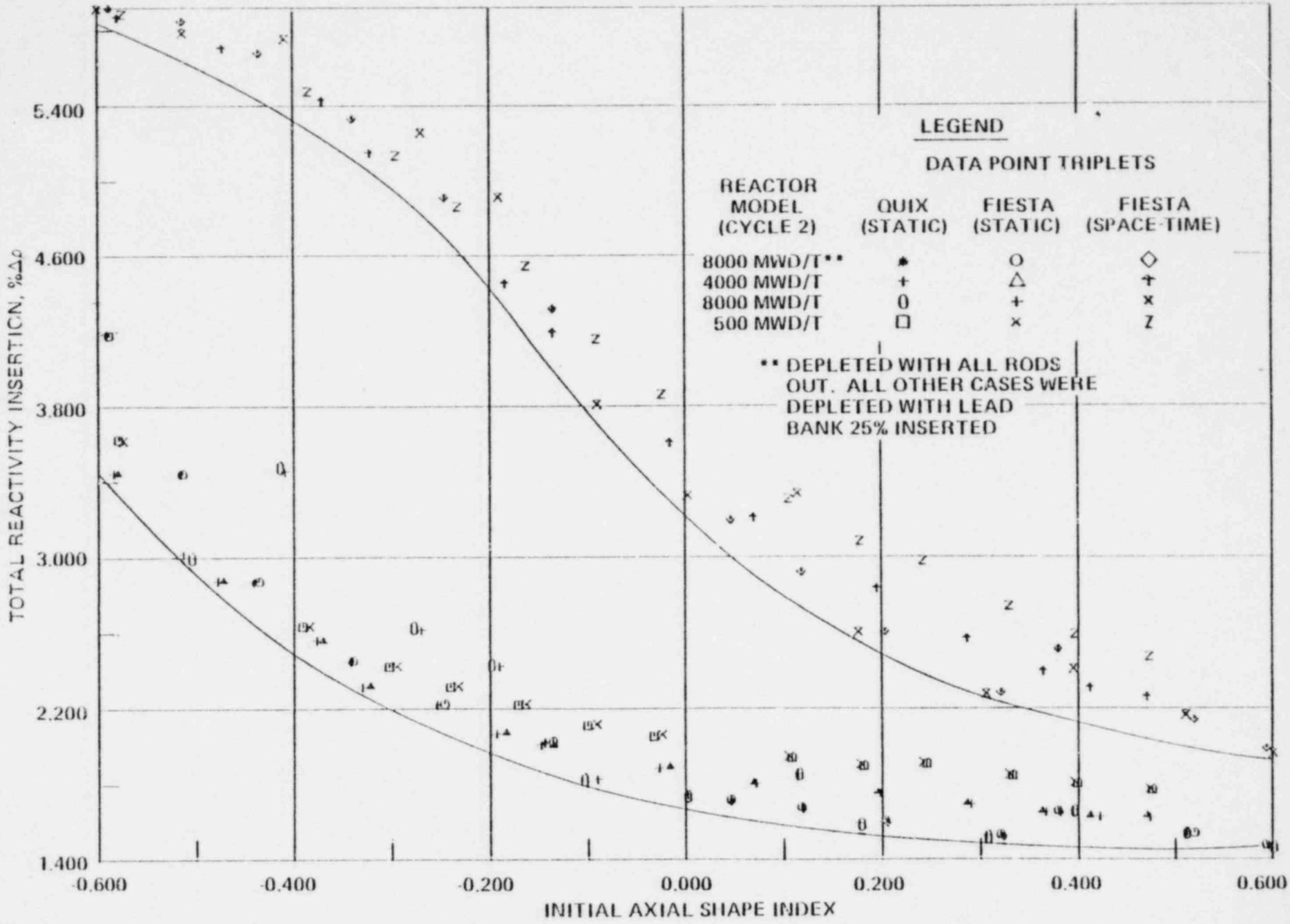

Figure 5.7

RATIO OF THE REACTIVITY INSERTION FOR VARIOUS TOTAL ROD WORTHS
RELATIVE TO THE REACTIVITY INSERTED FOR A ROD WORTH OF 6% $\Delta\rho$
ROD INSERTION IS 20%

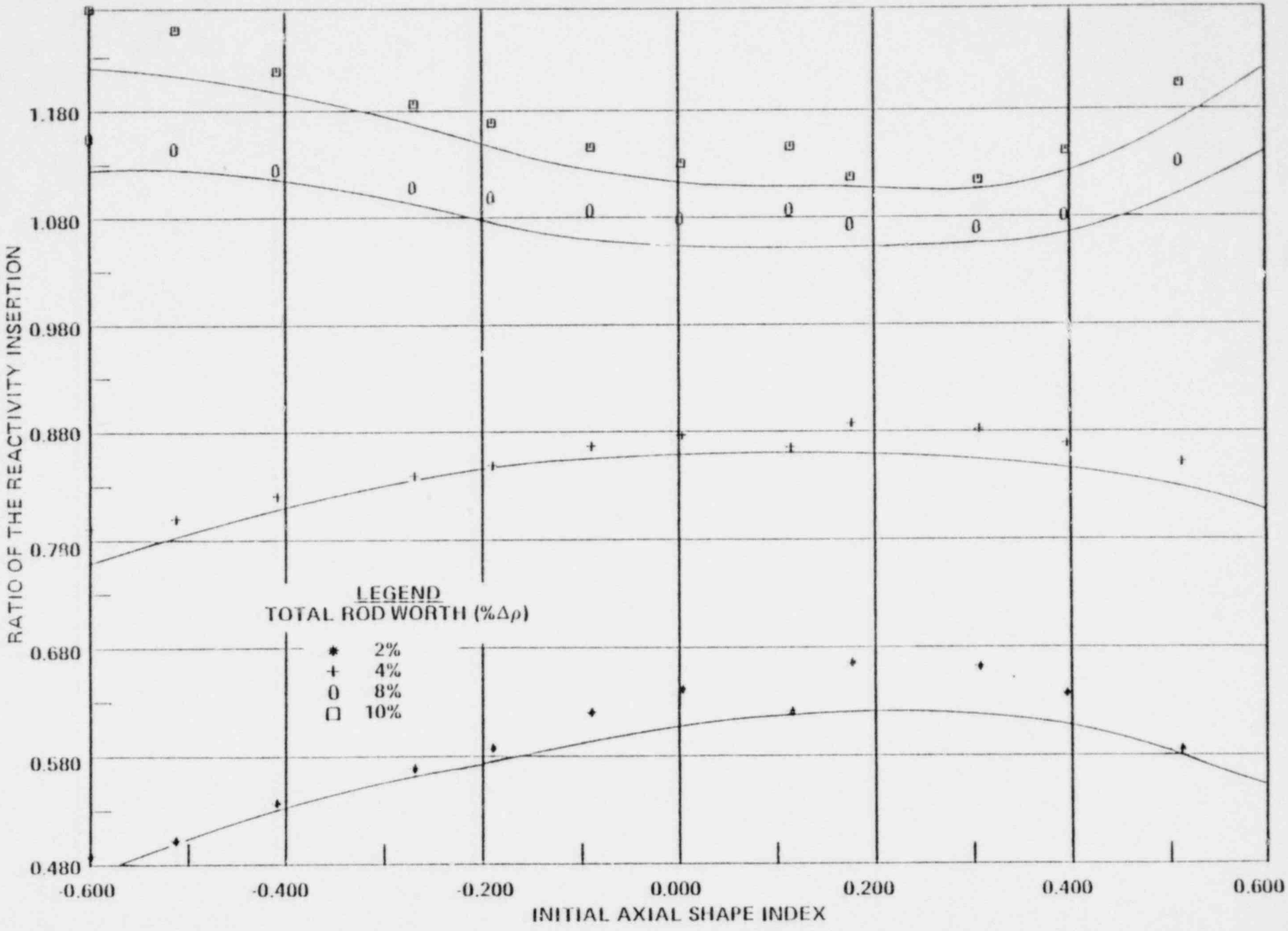

Figure 5.8

RATIO OF THE REACTIVITY INSERTION FOR VARIOUS TOTAL ROD WORTHS
RELATIVE TO THE REACTIVITY INSERTED FOR A ROD WORTH OF 6% $\Delta\rho$
ROD INSERTION IS 40%

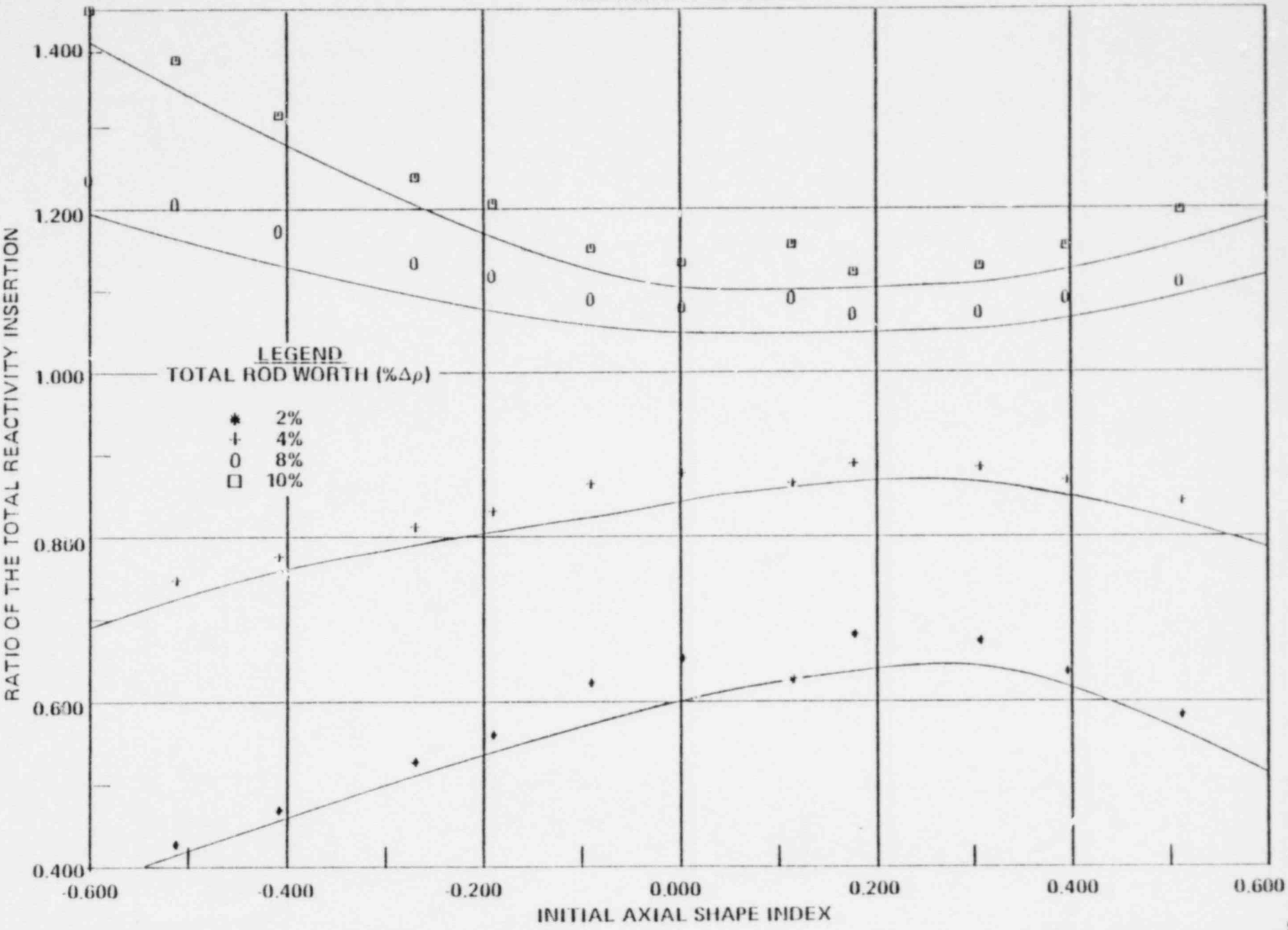

Figure 5.9

RATIO OF THE REACTIVITY INSERTION FOR VARIOUS TOTAL ROD WORTHS
RELATIVE TO THE REACTIVITY INSERTED FOR A ROD WORTH OF 6% $\Delta\rho$
ROD INSERTION IS 60%

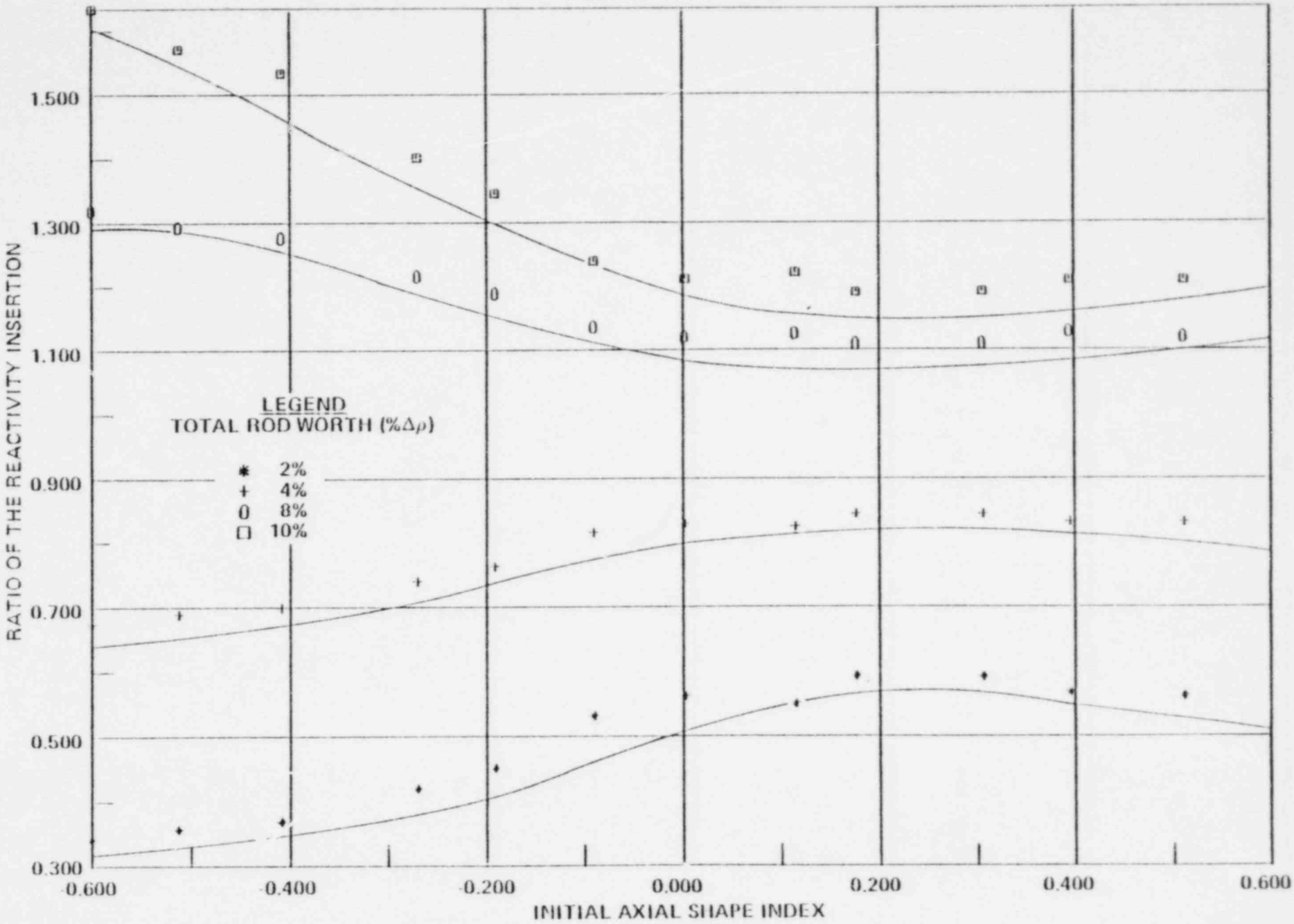

Figure 5.10

RATIO OF THE REACTIVITY INSERTION FOR VARIOUS TOTAL ROD WORTHS
RELATIVE TO THE REACTIVITY INSERTED FOR A ROD WORTH OF 6% $\Delta\rho$
ROD INSERTION IS 80%

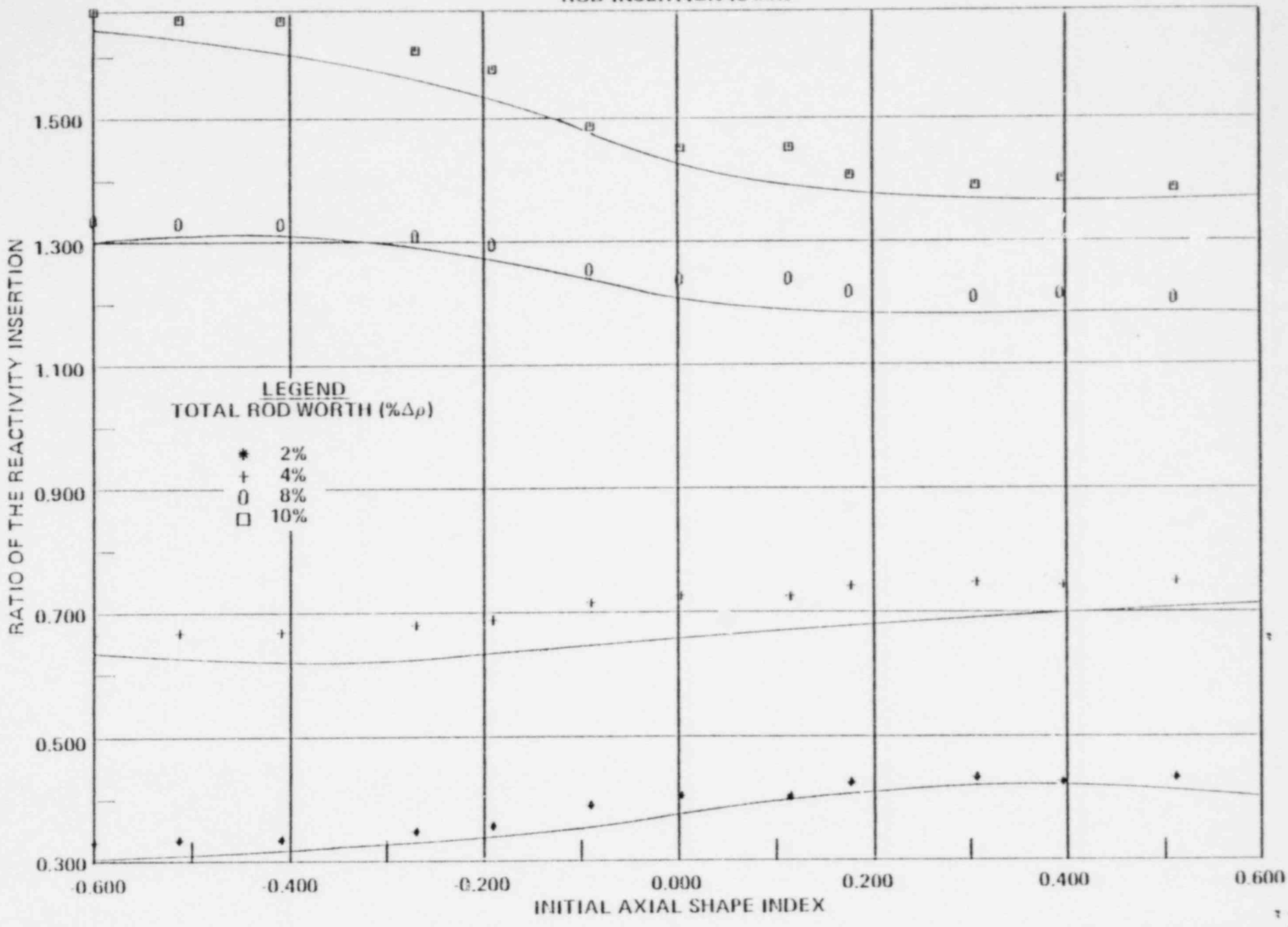

APPENDIX A

FIESTA Code - Input Description

Namelist if used for input of all data except the title. The title may consist of only one card, and for steady state continuation cases it must immediately follow the namelist arrays of previous steady state cases with a punch in column 1. For all cards except the title card the first column of every card must be blank.

1) Title 80 characters (The first character must non-blank for continuation cases, a "+" indicates new input is added to reference case input, otherwise all input must be respecified for new reference case)

2) $FIESTA

3) Array name KNTL

(1) - number of meshblocks - NOPTS ($\leq$100)

(2) - left boundary condition - IBCL

0 = Zero Flux
1 = Zero Current

(3) - right boundary condition - IBCR

(4) - geometry of neutron flux solution - IGEOM

0 - slab
1 - cylinder
2 - sphere

(5) - type of flow - ITYPE

0 - no flow
1 - parallel to neutron solution
2 - perpendicular to neutron solution

(6) - number of delayed neutron precursors (up to six are allowed) - IDELAY

(7) - number of perturbable rods ($\leq$20) - NRODs

(8) - number of time steps (no limit) - NTS

(9) - number of changes in the time step length - NPT ($\leq$20)

(10) - 0, 1 for short or long edit. - NEDIT (0 is recommended with detailed print specified by MPRINT)

(11) - cross section feedback functions - NFEEDY

0 - linear cross section variation with feedback variables
1 - special functional relation between cross sections and feedback variables

(12) - type of control rods - NRTYPE

0 - top entry rods
1 - bottom entry rods (applies only when flow is parallel to neutron solution)

(13) - mesh point at which cross sections are calculated for input checking purposes - NFMAC (for NFMAC = 0, no cross section check edits)

(14) - type of DNB calculation - NDNB (ITH = 1)

0 - none (used for this application)
1 - Janssen Levy
2 - TONG (W-3)

(15) - 0 - adjoint calculated for every steady-state case
1 - adjoint calculated only for the first steady-state case transient is allowed from only the first steady state case if KNTL(15)=1) (Default value = 0)

(16) - time dependent reactivity table - NRHO

0 - no
1 - yes

(17) - number of mesh intervals in the fuel pellet for thermal calculation - NFUEL (Ignore unless ITH = 1)

(18) - number of mesh intervals in the clad - NCLAD (NFUEL+NCLAD $\leq$ 18) (if either of the above are less than one, the code switches to a homogeneous thermal pin model) (Ignore unless ITH = 1)

(19) - 0 - normal feedback (default value)
1 - Skip Feedback calculation for transient solution or calculate Feedback for only the first steady state calculation

(20) - 0 - no burnout (heat transfer coefficient for film boiling is not used)
1 - with burnout (IDNB) (Ignore if NDNB = 0)

(21) - feedback option - ITH
0 - simplified feedback model based on enthalpy and homogeneous fuel pin model with no two phase flow calculation (TWIGL Model)
1 - feedback model with detail fuel pin model and 2 phase flow.

(22) - number of input values for time dependent inlet enthalpy table - ITHIN $\leq$100 (if 0 temperature (°F) instead of enthalpy is input)

(23) - number of input values for time dependent inlet flow table - ITFLW $\leq$20

(24) - number of input values for time dependent boron table - ITBOR $\leq$20

(25) - number of input values for time dependent pressure table ITPRS

(26) - sub-cooled void model - IVOID (ITH = 1)

0 - fog flow model
1 - Tong model with subcooled boiling

(27) - film coefficient correlation for boiling - IBøIL (ITH = 1)

0 - Jens Lottes
1 - Thom

(28) - flux guess - IGUESS

0 - none
1 - use input value or (for continuation cases) previously computed value

(29) - punch option - NPUNCH

0 - no
1 - yes

(30) - point kinetics option - NPTKIN

0 - no
1 - yes (bypasses flux shape calculation during transient)

(31) - number of load demand values for time dependent tables - IDMD $\leq$20

(32) - recirculation option (ICIRC)

0 - no
1 - yes (inlet enthalpy is calculated based on time delayed load and outlet enthalpy)

(33) - axial power shape for void model (for ITYPE = 2)

1 - uniform
2 - cosine

(34) - axial weighting of void (for ITYPE = 2)

1 - uniform
2 - cosine

(35) - for transverse flow (ITYPE = 2), the mesh interval at which axial thermo-hydraulic edits are desired - ITR

(36) - for transverse flow (ITYPE = 2) the number of axial nodes for integration of the void correlation - IAXIAL (default value = 40)

4) Array name PR

(1) - inverse fast velocity (sec/cm) - V1

(2) - inverse thermal velocity (sec/cm) - V2

(3) - integral convergence criterion - EPSE (10E-6 default value)

(4) - inlet system temperature - TIN* (for inlet enthalpy use minus sign (°F or BTU/lb)

(5) - system pressure (psia)* - PRES

(6) - thermo-hydraulic fuel rod - DE equivalent diameter (ft.)

(7) - fuel density in either lb/ft^3 or fract. of theoretical density of 683.4 lb/ft^3 - FDENS

(8) - initial core flow rate* - WZERO (lb/hr)

(9) - power dip in the center of the pin; power is distributed according to a parabolic fit - PDIP (ITH = 1)

(10) - initial boron concentration* (PPM) - BORO

(11) - fraction of the pin power which is generated directly in the clad - PCLAD (ITH = 1) (power generated in clad = PCLAD* (1-FRAC(I))* P(I)

(12) - convergence criteria for the thermo-hydraulic equations - EPSSO (ITH = 1)

(13) - reactor steady state power (MWT) - PZERO

*For time dependent variations of these parameters the above values are the initial values which are automatically placed in the tables as the time-zero entry.

(14) - cross sectional area of the reactor (cm^2) - SCAREA (axial problems)

(15) - height of the reactor - HIGH (radial problems) (cm)

(16) - depth of the reactor - WIDE (slab problems) (cm)

(17) - reference water density - REFDR (this value is only used to calculate cross sections of control rods for input checking purposes) (lb/ft^3)

(18) - fuel pellet radius (cm) - RPELLET (ITH = 1)

(19) - radial gap thickness (cm) - TGAP (ITH = 1)

(20) - clad thickness (cm) - TCLA (ITH = 1)

(21) - pointwise convergence criterion - EPSP (defaults to 100 X EPSE)

(22) - water density for cross section calculation for input checking purposes - (lb/ft^3) - RHOW1

(23) - same as above - RHOW2

(24) - same as above - RHOW3

(25) - same as above - RHOW4

(26) - reactor scram power (MWT) - PSCRAM (rod scram is initiated where the power exceeds this value)

(27) - fuel temperature for cross section calculation for input checking purposes (°F) - TEMP1

(28) - same as above - TEMP2

(29) - same as above - TEMP3

(30) - same as above - TEMP4

(31) - velocity coefficient of the scram rods ASCRAM (cm/sec)

(32) - velocity coefficient of the scram rods - BSCRAM (cm/sec)

rod position = (ASCRAM) * t + (BSCRAM) $*t^2$

(33) - maximum change in the amplitude function (default = 10) between flux shape recalculations - RMAX

(34) - minimum time step (default .001 sec) - this value is only used if a very small time step is calculated when PR(33) is near unity. Otherwise it is not used.

(35) - velocity coefficient of the scram rods in a second time interval - ASCRAM2

(36) - same as above - BSCRAM2

(37) - reference boron concentration - REFBOR

(38) - reference water density for boron input cross sections - DENS1

(39) - reference water density for boron input cross sections - DENS2

(40) - gap conductance limit - GPLIM (BTU/ft^2 F hr)

(41)*- water volume between outlet of the reactor and the load (FT3) - VOL1 (ICIRC = 1)

(42)*- water volume between outlet of the reactor and the inlet of the reactor (FT3) - VOL2 (ICIRC = 1)

(43) - fraction of non-moderator volume which is fuel - FUELRF (default = 1.0)

(44) - volume of the reactor inlet plenum (FT3) - VOLPLN ideal mixing is assumed to occur with the water entering the plenum; this model is used to calculate the inlet enthalpy only (for ICIRC = 1)

---

*These volumes are used to calculate the flow time delay by the following formula:

$$\tau = 3600 * V^* / W_c$$

The density is computed from the inlet enthalpy; the volume therefore need not be the actual physical volume (as in steam lines for example) as long as T is computed correctly. The input volume should be as follows:

$$V = V^1 \frac{\rho^1}{\rho} \frac{W_c}{W^1}$$

where V^1 ρ^1 and W^1 are the actual volume, density and flow in the pipe
ρ is the density at core inlet conditions
W_c is the core flow rate

5) Array name BETA (I = 1, IDELAY)

Delayed neutron fraction for each precursor group.

6) Array name LAMD (I = 1, IDELAY)

Decay constants of the delayed precursors (sec^{-1}).

7) MESH I = 1, NOPTS

special mesh intervals (cm)

8) BUKF I = 1, NOPTS

pointwise transverse fast buckling (cm^{-2})

9) BUKS I = 1, NOPTS

Pointwise transverse thermal buckling (cm^{-2})

The following are all pointwise arrays

I = 1, NOPTS

10) RD1 reference group one diffusion constant

11) RA1 reference group one absorption cross section

12) RR reference removal cross section

13) RNF1 reference nu sigma fission in group one

14) RF1 reference sigma fission in group one

15) RD2 reference thermal diffusion constant

16) RA2 reference thermal absorption cross section

17) RNF2 reference thermal nu sigma fission

18) RF2 reference thermal sigma fission

The following are the feedback definitions if NFEEDY = 0
(if all the following are zero no feedback is performed)
I = 1, NOPTS

19) DD1 pointwise change in D_1, per change in moderator density ($cm/g/cm^3$)

20) DA1 same for Σ_{a1}

21) DR same for Σ_r

22) DNF1 same for $\nu\Sigma_{f1}$

23) DD2 same for D_2

24) DA2 same for Σ_{a2}

25) DNF2 same for $\nu\Sigma_{f2}$

26) DD1DF pointwise change in D_1 per change in the square root of the absolute fuel temperature (cm/°R)

27) TA1 same for Σ_{a1}

28) TR same for Σr

29) TNF1 same for $\nu\Sigma_{f1}$

The following are the feedback definitions if NFEEDY = 1
I = 1, NOPTS

<u>the following functions are used</u>

FUNCTION

1) $\Sigma = a + b\rho + c\sqrt{T} + d\rho\sqrt{T}$

2) $\Sigma = a + b \ln(\rho + \rho o)$

3) $\Sigma = a + b\sqrt{T} + c \ln(\rho + \rho o) + d\sqrt{T} \ln(\rho + \rho o)$

where ρ = water density in g/cm^3 for all functions the value of a, b, c and d is computed from the reference cross sections

30) DD1DF pointwise value of constant "b" in equ. 3 for D_1

31) DD1 "c" equ. 3 for D_1

32) DD1DQ "d" equ. 3 for D_1

33) DD1DR (g/cc) "po" equ. 3 for D_1

34) TA1 "b" equ. 3 for Σ_{a1}

35) DA1 "c" equ. 3 for Σ_{a1}

36) DS1DQ "d" equ. 3 for Σ_{a1}

37) DS1DR (g/cc) "ρo" equ. 3 for Σ_{a1}

38) DR "b" equ. 1 for Σ_r

39) TR "c" equ. 1 for Σ_r

40) DRDQ "d" equ. 1 for Σ_r

41) DNF1 "c" equ. 3 for $\nu\Sigma_{f1}$

42) TNF1 "b" equ. 3 for $\nu\Sigma_{f1}$

43) DNF1DQ "d" equ. 3 for $\nu\Sigma_{f1}$

44) DNF1DR "ρo" (g/cc) equ. for $\nu\Sigma_{f1}$

45) DD2 "b" equ. 2 for D_2

46) DD2DR "ρo" equ. 2 for D2

47) DA2 "b" equ. 2 for Σ_{a2}

48) DS2DR "ρo" equ. 2 for Σ_{a2}

49) DNF2 "b" equ. 2 for $\nu\Sigma_{f2}$

50) DNF2DR "ρo" equ. 2 for $\nu\Sigma_{f2}$

Control Rod Cross Sections

The following functions are used to evaluate control rod cross sections

1) $\Delta\Sigma = a + b \ln (\rho + \rho o)$

2) $\Delta\Sigma = a + \rho + c\,\rho^2$

51) RODO1 rodwise value of "a" in equ. 1 for ΔD_1 I = 1,NrøDS

52) D1FROD "b" equ. 1 for ΔD_1

53) D2FROD "ρo" equ. 1 for ΔD_1

54) RODS1 "a" equ. 1 for $\Delta\Sigma_{a1}$

55) A1FROD "b" equ. 1 for $\Delta\Sigma_{a1}$

56) A2FROD "ρo" equ. 1 for $\Delta\Sigma_{a1}$

57) RODR "A" in equ. 2 for $\Delta\Sigma_r$

58) R1FROD "b" in equ. 2 for $\Delta\Sigma_r$

59) R2FROD "c" in equ. 2 for $\Delta\Sigma_r$

60) RODNF1 "a" in equ. 2 for $\Delta v\Sigma_{f1}$

61) F1FROD "b" in equ. 2 for $\Delta v\Sigma_{f1}$

62) F2FROD "c" in equ. 2 for $\Delta v\Sigma_{f1}$

63) RODD2 "a" in equ. 1 for ΔD_2

64) D1SROD "b" equ. 1 for ΔD_2

65) D2SROD "ρo" equ. 1 for ΔD_2

66) RODS2 "a" equ. 1 for $\Delta\Sigma_{a2}$

67) A1SROD "b" equ. 1 for $\Delta\Sigma_{a2}$

68) A2SROD "ρo" equ. 1 for $\Delta\Sigma_{a2}$

69) RODNF2 "a" equ. 1 for $\Delta v\Sigma_{f2}$

70) F1FROD "b" equ. 1 for $\Delta v\Sigma_{f2}$

71) F2FROD "ρo" equ. 1 for $\Delta v\Sigma_{f2}$

72) RDWGT rodwise weighting factor; all macroscopic control rod cross sections are multiplied by this value; this allows easy calibration of each rod to the measured value

73) POSINT rodwise initial position of the tip of the rod from the bottom of the core (cm)

for ITYPE = 1 and NRTYPE = 0
the rod cross sections are overlayed between POSINT and the top of the core

for ITYPE = 1 and NRTYPE = 1
the rod cross sections are overlayed between POSINT and the bottom of the core

74) NESHLT - left and right intervals
MESHRT - boundary for rod overlay when ITYPE = 2 the fraction of rod (k) which is inserted is equal to 'POSINT (K) - HIGH)/HIGH

75) TSTART - time (sec) at which the rod (k) starts moving; negative value indicates time delay for scram rods

76) RODRAT
(1) linear velocity coefficient of rod 1
(2) quadratic velocity coefficient of rod
(3) linear velocity coefficient of rod 2
(4) quadratic velocity coefficient of rod 2
etc. (2 x NRODS values $\leq$40)

77) TSTART2 - time (sec) at which the rod (k) starts moving according to the following coefficients, for scram rods this is a time delay

78) RØDRAT2 - velocity coefficients in the second time interval K - 1, 2 . . . . . 2 x NRODS $\leq$40

79) DIST - the maximum distance (cm) that each rod is allowed to move

80) TMSTEP - time step in seconds (NPT values $\leq$20)

81) NOSTEP - time limit (sec) to which TMSTEP applies (NPT values $\leq$20)

82) CVOL - pointwise coolant volume fraction 0<CVOL<1.0

83) AREA - pointwise heat transfer area divided by coolant volume (ft^{-1}) (for detailed fuel pin thermal model this quantity is computed)

AREA (I) = 60.96 (1 - CVOL (I))/(CVOL (I) $*R_{clad}$)

R_{clad} = clad outside radius (cm)

84) COND - point wise gap conductance BTU/hr ft^2 °F

if a homogeneous fuel pin model is used, this value is the overall conductance

if a detailed fuel pin model is used, this value need not be specified; however, if it is specified, it overrides the calculated value of the gap conductance

85) FRAC - pointwise fraction of the power which is generated directly in the coolant

86) RTF - pointwise reference fuel temperature (°F)

87) RDEN - pointwise reference coolant density (lb/ft^3)

88) HINTAB - inlet enthalpy (BTU/lb), input table (or temperature (°F) for KNTL(22) < 0)
TMHIN - time (sec)

89) FLWTAB - inlet flow (lb/hr) table
TMFLW - time (sec)

90) BORTAB - Boron (PPM) table
TMBOR - time (sec)

91) PRSTAB - pressure (psia) table
TMPRS - time (sec)

92) DMDTAB - load demand table (fraction of initial)
THDMD - time (sec)

93) D1BOR1
A1BOR1
RBOR1 pointwise change in macroscopic
NF1BOR1 parameters for
D2BOR1 reference boron concentration
A2BOR1 at water density (DENS1)
NF2BOR1

94) D1BO2
A1BOR2
RBOR2 pointwise change in macroscopic
NF1BOR2 parameters for reference boron
D2BOR2 concentration at water
A2BOR2 density (DENS2)
NF2BOR2

95) NPRINT - for NEDIT = 0 this array specifies the time points at which a detailed print is desired

If MPRINT(1) = -KK signifies a detailed print every KKth time step

96) FLXS - thermal and fast flux guess
FLXF - for IGUESS = 1

97) last card of namelist has "$" anywhere except in column 1

A blank card must follow the input if a transient calculation is desired. If several transient calculations are to be performed, each case must be followed by a blank card. If only steady state cases are desired, no blank card should appear between cases.

For continuation cases, if a "+" appears in column one of the title card, only the changes need to be specified. If a "+" does not appear in column one, the entire input is initialized to zero and all the input values must be re-specified.